



UNIVERSITA' DEGLI STUDI DI VERONA

DIPARTIMENTO DI

SCIENZE CHIRURGICHE, ODONTOSTOMATOLOGICHE E MATERNO-INFANTILI

SCUOLA DI DOTTORATO DI

SCIENZE DELLA VITA E DELLA SALUTE

DOTTORATO DI RICERCA IN

SCIENZE CARDIOVASCOLARI

Con il contributo di

UNIVERSITA' DEGLI STUDI DI VERONA

CICLO/ANNO XXXII/2016

TITOLO

POSTMORTEM MICRO-CT FOR FETAL HEART:
A VALIDATION STUDY AGAINST CONVENTIONAL AUTOPSY

S.S.D. MED/11

Coordinatore: Prof. GIOVANNI BATTISTA LUCIANI

Firma _____

Tutor: Prof. GIOVANNI BATTISTA LUCIANI

Firma _____

Tutor: Dr.ssa LUCIA ROSSETTI

Firma _____

Tutor: Dott. CLAUDIO LOMBARDI




Firma _____

Dottorando: Dott.ssa CAMILLA SANDRINI

Firma _____

Quest'opera è stata rilasciata con licenza Creative Commons Attribuzione – non commerciale
Non opere derivate 3.0 Italia . Per leggere una copia della licenza visita il sito web:

<http://creativecommons.org/licenses/by-nc-nd/3.0/it/>

-  **Attribuzione** Devi riconoscere una menzione di paternità adeguata, fornire un link alla licenza e indicare se sono state effettuate delle modifiche. Puoi fare ciò in qualsiasi maniera ragionevole possibile, ma non con modalità tali da suggerire che il licenziante avalli te o il tuo utilizzo del materiale.
-  **Non Commerciale** Non puoi usare il materiale per scopi commerciali.
-  **Non opere derivate** —Se remixi, trasformi il materiale o ti basi su di esso, non puoi distribuire il materiale così modificato.

*POSTMORTEM MICRO-CT FOR FETAL HEART:
A VALIDATION STUDY AGAINST CONVENTIONAL AUTOPSY*

Camilla Sandrini
Tesi di Dottorato
Verona, 05/12/2019

SOMMARIO

Obiettivo: la diagnosi prenatale precoce di cardiopatia congenita è oggi giorno possibile. La valutazione postmortem del cuore fetale riveste un ruolo importante per il counselling familiare e per scopi di educazione medica e di ricerca. L'autopsia convenzionale, fino ad oggi considerata il gold standard, è gravata da numerose limitazioni. Pertanto, sono state proposte metodiche alternative. L'obiettivo dello studio è di valutare l'accuratezza diagnostica della postmortem micro-CT per la definizione delle strutture cardiache fetali del primo e secondo trimestre.

Materiali e metodi: dopo interruzione volontaria di gravidanza, i campioni contenenti il cuore fetale sono stati sottoposti a micro-CT e successivamente ad autopsia convenzionale. L'approccio segmentario è stato utilizzato per definire le strutture cardiache. Ventisei indici di anatomia cardiaca sono stati utilizzati per analizzare ogni campione con entrambe le tecniche e per confronto. In prima analisi, il gold standard è stato definito l'autopsia convenzionale. In seconda analisi, il gold standard è stato considerato la micro-CT.

Risultati: sono stati collezionati 55 casi (epoca gestazionale 17.0 ± 2.9 settimane, range 12^{+5} - 21^{+6}). L'analisi è stata effettuata su 48 casi, di cui 29 (60.4%) affetti da cardiopatia congenita e 24 (50%) provenienti da precoce interruzione volontaria di gravidanza ("challenging specimens"). La micro-CT era diagnostica in tutti i casi mentre l'autopsia convenzionale non era in grado di definire alcuna struttura cardiaca in 11 casi (22.9%). Per l'analisi dell'end point primario (indice "visibile"/"non visibile") e secondario (indice "normale"/"anormale"/"non diagnostico"), concordanza, sensibilità, specificità, potere predittivo positivo e negativo erano alti sia nella popolazione generale sia nella popolazione di "challenging specimens". L'86.1% ed il 91.3% degli indici definiti "non diagnostici" dall'autopsia convenzionale sarebbe stato visibile dalla micro-CT nella popolazione generale e nel sottogruppo di "challenging specimens", rispettivamente. Considerando la micro-CT come tecnica gold standard, sensibilità e potere predittivo negativo erano bassi nell'analisi dell'end point primario. Solo il 13.9% e l'8.5% degli indici definiti "non diagnostici" dalla micro-CT sarebbe stato visibile dall'autopsia convenzionale nella popolazione generale e nel sottogruppo di "challenging specimens", rispettivamente. Il 60.1% degli indici "non diagnostici" apparteneva al sottogruppo di "challenging specimens". Considerando l'autopsia come gold standard, la micro-CT avrebbe aggiunto il 23.3% ed il 31.3% di informazioni alla diagnosi posta dall'autopsia nella popolazione generale e nel sottogruppo di "challenging specimens". Considerando la micro-CT come gold standard, l'autopsia convenzionale avrebbe aggiunto il 3.8% ed il 2.9% di informazioni alla diagnosi posta dalla micro-CT nella popolazione generale e nel sottogruppo di "challenging specimens".

Conclusioni: la postmortem micro-CT rappresenta una valida alternativa all'autopsia convenzionale per la valutazione postmortem del cuore fetale sia nel primo trimestre sia nel secondo trimestre. Essa è superiore al gold standard per la valutazione dei campioni provenienti da interruzioni di gravidanza precoci. Essa può colmare i limiti dell'autopsia convenzionale per la valutazione dei cuori di

piccole dimensioni, rispondendo alla necessità clinica di avere un'adeguata valutazione ex-vivo dei cuori provenienti da interruzioni di gravidanza o aborti spontanei precoci.

ABSTRACT

Aims: Early prenatal diagnosis of congenital heart disease is feasible. Post-mortem examination of the fetal heart is important for familial counselling, educational and research purposes. Conventional autopsy, the current gold standard technique for post-mortem confirmation, has numerous limits. Alternative radiologic techniques have been proposed. The objective of the study is to evaluate the diagnostic accuracy of post mortem micro-CT as compared to conventional autopsy for the definition of heart structure in early and late gestation human fetal cardiac samples.

Material and methods: Ex-vivo human fetal hearts underwent evaluation by micro-CT and conventional autopsy. Segmental approach was used to define cardiac structures. Twenty-six indices of cardiac anatomy were analyzed by both technique for each case and were used for comparison. We considered firstly conventional autopsy and secondly micro-CT as gold standard technique.

Results: Fifty-five cases were collected (gestational age 17.0 ± 2.9 weeks, range 12^{+5} - 21^{+6}). Forty-eight cases were analyzed. CHD were present in 29 out of 48 cases (60.4 %). Twenty-four cases (50%) belong to the group of “challenging specimens”. Micro-CT was conclusive in all cases while conventional autopsy could not evaluate any cardiac structures in 11 out of 48 cases (22.9%). For the analysis of primary (definition of indices as “visible”/“non-visible”) and secondary end point (definition of indices as “normal”/“abnormal”/“non-diagnostic”), sensitivity, specificity, positive and negative predictive value were high in both general population and in the subgroups of “challenging specimens”. 86.1% and 91.3% of indices defined “non-diagnostic” at conventional autopsy would be visible by micro-CT in general population and in the subgroup of “challenging specimens, respectively. When using micro-CT as gold standard technique, sensitivity and NPV were low in the analysis of primary end point. Only 13.9% and 8.5% of indices defined “non-diagnostic” at micro-CT would be visible by conventional autopsy in general population and in the subgroup of “challenging specimens, respectively. 60.1% of the “non-diagnostic” indices belong to the subgroup of “challenging specimens”. Considering autopsy as gold standard technique, micro-CT would add 23.3% and 31.3% information to diagnosis made by autopsy in the general population and in the subgroup of “challenging specimens”. Considering micro-CT as gold standard technique, autopsy would add 3.8% and 2.9% information to micro-CT diagnosis in the general population and in the subgroup of “challenging specimens”.

Conclusion: Postmortem micro-CT represents a valid alternative to conventional autopsy for postmortem evaluation of human fetal heart coming from both early and late terminations of pregnancy. It is superior to conventional autopsy for the evaluation of samples coming from early termination of pregnancy. It bridges the gap of conventional autopsy for the evaluation of very small hearts and meets the clinical need of having a confirmation of first trimester prenatal fetal investigation after early termination of pregnancy or fetal demise.

ABBREVIATIONS

CHD: congenital heart disease

EUROCAT: European Surveillance of Congenital Anomalies

D-TGA: D-transposition of the great arteries

LVOTO: left ventricular outflow tract obstruction

HLHS: hypoplastic left heart syndrome

GA: gestational age

eFE: early fetal echocardiography

TOP: termination of pregnancy

Micro-CT: micro computed tomography

cMRI: cardiac magnetic resonance imaging

HREM: high resolution episcopic microscopy

T: Tesla

IVC: inferior vena cava

SVC: superior vena cava

CS: coronary sinus

PPV: positive predictive value

NPV: negative predictive value

NT: nuchal translucency

VSD: ventricular septal defect

TOF: tetralogy of Fallot

ASD: atrial septal defect

LV: left ventricle

PA-VSD pulmonary atresia/ventricular septal defect

AVSD: atrioventricular septal defect

RV: right ventricle

TA: tricuspid atresia

CNS: central nervous system

IUGR: intra uterine growth restriction
SVR: systemic venous returns
PVR: pulmonary venous returns
RA: right appendage
LA: left appendage
TV: tricuspid valve
MV: mitral valve
RVOT: right ventricular outflow tract
LVOT: left ventricular outflow tract
PV: pulmonary valve
MPA: main pulmonary artery
RPA: right pulmonary artery
LPA: left pulmonary artery
AoV: aortic valve
Ao: aortic
AV: atrio-ventricular
VA: ventriculo-arterial
NC: not calculable
MAPCAs: major aorto-pulmonary collateral arteries
CI: confidence interval

INDEX

BACKGROUND	9
Prenatal diagnosis of congenital heart disease	9
Postmortem evaluation of heart disease	11
Post-mortem contrast-enhanced micro computed tomography	11
Post-mortem cardiac magnetic resonance imaging	13
Postmortem CT-angiography	13
High resolution episcopic microscopy	14
Synchrotron X-ray phase contrast imaging	14
Objective of the study	14
MATERIALS AND METHODS	16
Case selection and samples preparation	16
Micro-CT	16
Autopsy examination	17
Data analysis	17
Statistical analysis	18
RESULTS	20
Gold standard: autopsy	20
Gold standard: micro-CT	23
“Non-diagnostic” indices	25
DISCUSSION AND CONCLUSIONS	26
REFERENCES	28
TABLES	37
FIGURE LEGEND	54

BACKGROUND

Prenatal diagnosis of congenital heart disease

Heart defects are one of the most frequent congenital malformations, occurring about in 1% of liveborn and in a higher proportion in fetuses. They can be isolated or associated with other malformations, syndromes or chromosomal abnormalities (1,2). In the last decade, huge progresses in managing of congenital heart disease (CHD) prompted an overall better prognosis and a longer survival (3-8). Notwithstanding, cardiac malformations still significantly affect morbidity and mortality before birth, after birth and long-life. EUROCAT reports an overall prevalence of heart defects of 8‰ births (range 5.36-15.32‰), of which 12% are associated with chromosomal anomalies. Perinatal mortality is significantly linked to heart malformations: in 2004 in Europe, about 6% of early neonatal deaths were related to heart defects (9). Even if prenatal diagnosis of CHD should intuitively always carry better outcome, its impact on outcome is still a matter of debate. Prenatal diagnosis seems to reduce neonatal morbidity and, to a lesser extent, neonatal mortality for at least some specific type of CHD (D-transposition of the great arteries [TGA], aortic coarctation, left ventricle outflow tract obstruction [LVOTO], hypoplastic left heart syndrome [HLHS], ductal dependent lesions) because it predicts the need for urgent drug infusion or emergent postnatal intervention allowing rapid stabilization of the postnatal circulation and avoiding neonatal critical transport to tertiary Centre (10-18). Studies documenting improved mid and long term survival are sparse (10). Global detection rate of CHD in utero is about 60-85% and it is influenced by acoustic window, fetal position, dimension of the heart and vasculature structure and specific characteristic of feto-placental circulation (18-24). Embryology of human fetal heart is an expansive field of research. Cardiovascular system is the first that develops during embryogenesis. Indeed, heart formation starts at the end of the 3rd – beginning of the 4th week gestational age (GA) from a simple tube, when static diffusion is no longer able to provide satisfactory nutritional support to embryo's tissue, and is generally completed between the 7th-8th week GA. At the end of the 5th month, most of the structures are anatomically completed even if they continue to mature throughout fetal and perinatal life. Heart formation implies complex processes of primary myocardium differentiation into chamber myocardium in some regions, of chamber myocardium differentiation along cranio-caudal, dorso-ventral and left-right axis, of septation and loop of initial single cavity and of initial single trunk (25-27). Early prenatal diagnosis of CHD is nowadays feasible, thanks to progress in technology and to better understanding of risk factors for heart malformations. First trimester obstetric program of screening for fetal aneuploidies based on nuchal translucency and anomalies of soft marker (i.e. nasal bone, pattern of flow in ductus venosus and tricuspid regurgitation) is nowadays routinely used. It allows highlighting a population of pregnancies at higher risk for CHD, chromosomal anomalies and extra-cardiac malformations. Invasive genetic testing, second level ultrasound examination and early fetal echocardiography (eFE) can be offered to this population (28-36). eFE should be performed by trained physicians in order to correctly define cardiac malformations and to estimate prognosis in familial counselling.

The approach to studying the heart is similar to that used later in pregnancy. Sequential segmental analysis is the recommended schema. Transverse sections are used to define the abdominal situs, the four chamber view, the outflow tracts and three vessel view. Sagittal planes are performed to define aortic and ductal arch, bicaval view and short axis view of the ventricle and atrioventricular valve. Proper heart visualization is quite always possible early in gestation by trans-abdominal probe (37-40). Persico and coll demonstrated high accuracy (93.1%) of 11-13 weeks fetal cardiac evaluation when performed by well-trained physicians (38). As compared to second trimester scanning, definition of cardiac structure in first trimester relies more on color Doppler techniques. Hutchinson et al (39) performed eFE on 261 fetuses (GA 10⁺⁶ weeks, range 6⁺¹-13⁺⁶). Successful assessment of four chamber view could be achieved in 52% at 8 weeks GA, 80% at 10 weeks GA and 98% after the 11th week GA. Outflow tracts could be visualized in 4% of cases by 2D imaging at 8 weeks GA and in 72% at 11 weeks GA. Aortic and ductal arch could be defined in 28% of cases by 2D imaging. By combining 2D and color Doppler technique, their identification reached 58% at 10 weeks GA and 90% at 12 weeks GA. Inferior vena cava was visualized in 4% and 80% of cases by 2D technique and 2D+color Doppler technique, respectively, at 8 weeks GA. Its identification increased to 13% at 10 weeks GA and 80% after the 13th week GA. Evaluation of pulmonary veins remains challenging early in pregnancy, becoming possible in all cases after the 15th week of gestation. Care must be taken when early assessing fetal heart. Hemodynamic characteristics are peculiar in first trimester. Doppler technique shows lower ventricular compliance and short ventricular relaxation time through uniphasic ventricular inflow pattern at mitral or tricuspid sampling, significant a-wave reversal in systemic veins and ductus venosus, umbilical vein pulsation, lack of diastolic flow in the umbilical artery and tele-diastolic anterograde flow in great vessels. Moreover, even if global anatomy of the heart is the same as in the second trimester, early in gestation the cardio thoracic ratio is higher, the cardiac axis is more midline and it shifts leftwards to reach its definitive position at about 45° at 12 week GA, atrial chambers are larger as compared to the rest of cardiac mass, pericardial effusion is common and offset of atrioventricular valves can be difficult to be identified, leading to false diagnoses of atrioventricular septal defect. Even more so than in mid-gestation, the ventricular size and the dimension of great arteries should be symmetrical, with pulmonary trunk only slight larger than aortic vessel. Minor differences in their size can be indicative of pathology, raising suspicion of evolutive disease and highlighting the need for serial reassessment (39-40). Early diagnosis of congenital heart disease is important for familial counselling, clinical and research purposes. On one hand, it promotes the research of possible associated extra-cardiac and chromosomal anomalies, it allows physicians to study the progression of the disease in order to potentially offer earlier in utero intervention and it provides time for extensive prenatal counseling, family support and delivery planning. On the other hand, advancements in fetal imaging technology ameliorate medical knowledge of prenatal course of heart disease (40-42).

Postmortem evaluation of heart disease

Diagnosis of fetal malformations and/or chromosomal anomalies can lead to parental decision for termination of pregnancy (TOP). Post-mortem examination of the fetal heart is important for familial counselling, educational and research purposes. Conventional autopsy is the current gold standard technique for ex-vivo confirmation of CHD, despite its invasive and destructive features. Autopsy rate has significantly dropped in the last decades due to cultural, economics and medical factors. Cannie et al showed that, according to English law, familial refusal of conventional autopsy depends mainly on factors over which medical staff has no control, such as religion (muslin mothers accept it in about 40% of cases, as compared to 70% of non-Muslim), gestational age at TOP (the higher the gestational age, the lowest acceptance), the reason for TOP (higher acceptance was noted for fetal demise as compared to TOP for chromosomal anomalies and fetal malformations) and the medical staff who manage the counselling (fetal medicine specialist was associated to higher acceptance) (43). In the United States of America, changes in healthcare environment seem to play a role in the reduction of requested autopsy (44). Moreover, conventional autopsy can be challenging, up to impracticable, even for expert pathologists, especially in case of specimens low for GA, dimension or weight (45-47). Due to the relatively high rates of early termination of pregnancy in case of early diagnosis of fetal malformations, the number of challenging specimens is increasing and the limitations of conventional autopsy is nowadays an emerging problem for clinicians. To overcome known limits of conventional autopsy in post-mortem evaluation of fetal heart, different radiologic techniques have been proposed, such as post-mortem contrast-enhanced micro computed tomography (micro-CT) (48-63), post-mortem cardiac magnetic resonance imaging (cMRI) (48-50, 64-70), post-mortem CT-angiography (48,71), high resolution episcopic microscopy (HREM) (49, 72-74), synchrotron X-ray phase contrast imaging (48, 75-79) and three dimensional ultrasound technique (80). They may become valid alternative to autopsy for ex-vivo cardiac examination, especially in case where autopsy lacks of diagnostic power. Moreover, they may provide new insight into functional and electromechanical alterations in heart disease.

Post-mortem contrast-enhanced micro computed tomography

Post mortem micro-CT can easily define bone and mineralized structures. Conversely, vascular structures and soft tissues need contrast agent to be correctly identified. Preparation of specimens with contrast medium seems not to deform significantly organs and tissues. Micro-CT has been tested in ex-vivo murine hearts (53-58), in fetal and adult human cardiac samples (59-62) and in human fetal whole body (63), demonstrating promising results. Pioneering study in genetic modified mice, enriched in mutations causative of heart malformations, compared postmortem micro-CT to conventional autopsy. Samples were first fixed in formalin and then immersed in iodine solution for 48-72 hours before CT scanning. 2105 mice were studied, of which 380 pathological neonates and 41 pathological adults. Diagnostic accuracy, sensitivity and specificity for single type of CHD were analyzed. Postmortem micro-CT showed good sensibility (> 85%), except for small ventricular septal defects, valvar pathologies, coronary arteries and aortic arch abnormalities (difficult differential diagnosis between severe aortic

coarctation and interrupted aortic arch) (58). In 2014, Lombardi et al published a pilot study on feasibility of postmortem micro-CT on evaluating human fetal whole body and ex-vivo isolated hearts coming from 1st and 2nd trimester of pregnancy, comparing micro-CT (available for all cases) with conventional autopsy (available only for cases with GA > 13 weeks). Isotropic voxel size was 9 to 35 μm . Twenty-one samples were analyzed (7 whole bodies of GA 7-17 weeks, 14 isolated fetal hearts of GA 11-22 weeks, 6 prenatal diagnoses of cardiac malformation after the 15th week GA). The four chamber view, the crux cordis, the atrioventricular valves and the three vessel view were analyzed. Micro-CT was able to define cardiac anatomy in 3 cases where autopsy failed, was concordant with conventional autopsy in 6 cases and added anatomic details otherwise not evaluable by autopsy in 5 cases. In the last group, micro-CT defined the presence of atrioventricular septal defect in 2 cases and it differentiated between types of heart malformations in 3 cases. They preliminarily demonstrated that postmortem micro-CT could be used to study human fetal heart (59). In 2016, Hutchinson et al compared micro-CT to conventional autopsy by analyzing 6 human fetal hearts (5 CHD, 1 normal heart; GA between 17 and 23 weeks). Isotropic voxel size was 19 to 31 μm . They studied the heart by defining 21 indices of cardiac anatomy. Global concordance between micro-CT and conventional autopsy was 95.8%, sensitivity and specificity were respectively 85.2% and 98.9%, positive (PPV) and negative predictive values (NPV) were both 95.8%. They conclude that postmortem micro-CT provided accurate definition of CHD and seemed to be superior to autopsy for myocardial analysis and for evaluation of coronary arteries (60). Following these preliminary results on human fetal heart, Sandrini et al compared postmortem micro-CT to conventional autopsy in 10 fetal pathological hearts (GA 12⁺⁴-21⁺⁶ weeks) by applying cardiac segmental analysis. Isotropic voxel size was 9 to 18 μm . Each sample was analyzed by both techniques by studying 25 indices of cardiac anatomy. For comparable indices (174/250, 69.6%), agreement, sensitivity and specificity were 100%. Fifty out of 76 (65.7%) non-diagnostic indices belong to the subgroup of challenging specimens (GA < 16th week and weight < 1 g), of which 84 % (42/50) are evaluable by micro-CT but not by conventional autopsy (“apparent advantage of micro-CT”). Conversely, only 4% (2/50) indices were definable by autopsy but not by micro-CT (“missense of micro-CT”). Authors concluded that micro-CT could be a valid alternative to conventional autopsy for post mortem evaluation of human fetal heart and that it may prove superior to conventional autopsy, particularly in cases coming from early termination of pregnancy or in samples of small dimension or of low weight. Several limitations were present (small population; heterogeneity of samples, absence of normal hearts, and non-blinded comparison between techniques (61). Hutchinson et al evaluated the diagnostic accuracy of micro-CT for non-invasive whole body human fetal autopsy in 21 early gestation fetuses (GA 11-21 weeks). Isotropic voxel size was 7.4 to 51.0 μm . Forty indices were studied (7 neurologic, 10 thoracic, 9 cardiac, 13 abdominal, 1 musculo-skeletal). Overall, micro-CT agreed with autopsy finding in 35/38 diagnoses across 20 fetuses (agreement 100%, sensitivity 93.8%, specificity 100%). For comparable indices, there was full agreement for 700/718 (97.5%), sensitivity 89.7%, specificity 99%. When analyzing first trimester fetuses (\leq 14 weeks GA), micro-CT analysis yielded significantly fewer non-diagnostic indices

as compare to autopsy. Authors concluded that micro-CT had high concordance with conventional autopsy in early gestation fetuses, allowing to perform non-invasive autopsy with 92% diagnostic accuracy in fetuses at <22 weeks gestation (63).

Post-mortem cardiac magnetic resonance imaging

In 2012, Votino et al studied 24 samples of human fetal heart (median GA 15⁺³ weeks, range 11-20 weeks; median weight 51 g, range 4-310 g; 8 complex CHD, 2 simple CHD), comparing lower field (1.5-3 Tesla [T]) and higher field cMRI (9.4 T) with conventional autopsy. Lower field cMRI were able to define only cardiac situs and four chambers in 75% of samples of GA > 16 weeks. 9.4 T cMRI, at any GA, could define the four chamber view with a sensitivity of 66.7% and specificity of 80% and the outflow tracts with a sensitivity of 75% and specificity of 100%. Higher field cMRI allowed diagnosis of complex cardiac defects in 7 out of 8 cases (67). In 2014, Sandaite et al applied 3T cMRI to 24 cases of CHD (median GA 22 weeks, range 12⁺⁵-34⁺⁶ weeks). When GA was higher than 16 weeks, diagnostic accuracy was 54.5% for simple CHD and 92.3% for complex CHD. cMRI could not define valvar pathologies (68). In another study, radiologists with expertise in the field of post mortem MRI imaging of fetal heart applied high resolution sequences and 3D reconstruction to 1.5T cMRI and compared it with conventional autopsy. Four hundred cases were studied (185 fetuses of GA < 24th week, 92 fetuses of GA > 24th week, 123 death after birth before 16 years), of which 47 had cardiac malformations (20 fetuses of GA < 24th week, 5 fetuses of GA > 24th week, 22 cases in the last group). Overall, sensitivity, specificity, PPV and NPV were respectively 72.7%, 96.2%, 72.7%, 96.2%. Considering only complex CHD, sensitivity, specificity, PPV and NPV were respectively 92.6%, 99.1%, 89.3%, 99.4%. When analyzing the group dead after birth, sensitivity and NPV were lower as compared to general population, because of the presence of myocarditis (diagnosed only by histological study in conventional autopsy). Authors concluded that cMRI could be a valid alternative to conventional autopsy for neonates and children but, in case of normal heart, histological analysis was needed in order to exclude acquired muscular disease (69).

Postmortem CT-angiography

In 2012, Votino et al compared contrast-enhanced CT angiography with prenatal ultrasound and conventional autopsy. They studied 33 fetuses (median GA 25 weeks, range 18-39), of which 6 with prenatal suspected CHD. Injection of contrast agent was from umbilical cordon (8 cases) or intra-cardiac (25 cases). Cardiac situs, four chambers and outflow tracts were visualized in 87.9%. (29/33 cases). In the other ones, cardiac anatomy was not evaluable because of absence of contrast agent in the heart (umbilical approach in 3 cases, cardiac approach in 1 case). In case of prenatal diagnosis of heart disease, CT angiography missed 1 case and identified two ultrasound false negative cases (ventricular septal defect). There were no false negative cases on CT angiography. On multivariate analysis, ability to correctly identify cardiac anatomy correlated only to contrast cardiac injection (71).

High resolution episcopic microscopy

This technique need samples to be dehydrated and embedded in standard resin before undergo scanning by a modified microscope equipped with a digital video camera. Voxel size can reach 1 μm dimension. Gindes et all studied 30 human fetal heart samples (median GA 11⁺⁴ weeks, range 9⁺⁰-14⁺⁶), concluding that HREM was able to study the heart and to define specific cardiac features in the first trimester, such as prominent atrial appendage, small size atria, spiral ventricular arrangement, prominent coronary arteries and thickened arterial wall (73).

Synchrotron X-ray phase contrast imaging

Synchrotron X ray sources of energy allows imaging of formalin-fixed soft tissue without the need for contrast agent or sample sectioning. Additional component can be added to conventional X-ray sources to improve image quality. It is nowadays used only in research fields, where it represents an emerging technique. It has been applied to animal (75-77) and human (78,79) ex-vivo samples to define both structural heart changes and microscopic cardiac features. Increasing evidences are emerging regarding its ability to study the heart structure at microscopic details, including evaluation of the arrangement of myocytes within the myocardium, the location of conduction system and of coronary arteries. It may give unknown information to better understand functional and electromechanical properties of normal and pathological hearts.

Three dimensional ultrasound technique

In 2018, Votino et al compared post-mortem 2D and 3D echography with conventional autopsy on 88 fetuses (gestational age 11-40 weeks). Examiner was not blinded to prenatal information. Ultrasound resolution power was 0.5 mm. Each organ system was defined as normal, abnormal or not-diagnostic. The analysis of the heart consisted in the evaluation of the 4 chamber and the great vessels. The sensibility and specificity of ultrasound scan for the detection of thoracic anomalies (heart and lungs) were respectively 88.9% (95% CI, 65.3-98.6%) and 92.8% (95% CI, 84.1-97.6%). Echography failed to demonstrate one case of TOF and 1 case of perimembranous VSD. The Authors demonstrated the feasibility of post-mortem ultrasound for the purpose of virtual autopsy and showed that it had high sensibility and specificity in detecting congenital structural anomalies (80).

Objective of the study

The objective of the study is to evaluate the diagnostic accuracy of postmortem micro-CT as compared to conventional autopsy for the definition of heart structure in early and late gestation human fetal cardiac samples. The primary aim of the study is to define whether micro-CT is at least equal to conventional autopsy in post-mortem diagnosis of the global enrolled population. We hypothesize that CT has similar diagnostic strength as compared to autopsy. The secondary aim of the study is to define if micro-CT is at least equal, but even more accurate, to conventional autopsy in analyzing challenging samples (GA < 16 weeks and weight < 1 g). In this subgroup, we hypothesize that micro-CT has greater diagnostic power when compared to conventional autopsy.

MATERIALS AND METHODS

Case selection and samples preparation

The study has been approved by the local ethic committee as multicenter, experimental, double-blinded, two arms (normal pathological hearts) clinical trial (CE 1623). All samples were handled according to the Human tissue act (81). Fully informed, written women's consent for data treatment, imaging and use of tissue for research was obtained. Cases were recruited prospectively from two Centers between July, 2016 and July, 2019. Inclusion criteria consisted in: age \geq 18 years, presence of fetal echocardiography, decision for TOP, agreement to participate to study. Exclusion criteria consisted in age $<$ 18 years, absence of prenatal ultrasound, illegal TOP, insanity and psychiatric disorder, refuse to participate to study. For each case, we collected and anonymized prenatal data (GA at fetal echocardiography, GA at TOP, type of TOP, cardiac diagnosis, extra-cardiac findings and chromosomal anomalies, if any), micro-CT data (% Lugol, hours in Lugol, filter, spatial resolution, exposition time, voltage, current, rotational step) and macroscopic data (type and quality of samples, weight pre and post Lugol, transverse, longitudinal and antero-posterior diameter). Prenatal information were used for epidemiological description of the studied population. As conventional autopsy cuts samples and alters anatomic relationship between cardiac structures while micro-CT has no destructive nature, we decided to perform firstly micro-CT and secondly conventional autopsy. Samples consisted in isolated ex-vivo human fetal hearts or heart-lungs in case of prenatal suspicion of heterotaxy syndrome or in cases where pathologist deemed difficult to separate heart from lungs without affecting heart architecture. A single pathologist with expertise on fetal-placental disease isolated the samples. They were fixed in 10% formalin to prevent tissue degradation and remain in formalin in the time interval between isolation and micro-CT and between micro-CT and conventional autopsy.

We arbitrarily defined "challenging specimens" samples coming from early TOP (GA \leq 16th week) and of low weight (\leq 1 gram).

Micro-CT

Samples were removed from 10% formalin, weighted and immersed in contrast solution. Lugol was chosen as contrast agent and was prepared from 10 g potassium iodine and 5 g iodine in 100 mL water. The potassium iodide in water dissociates and the addition of elemental iodine induces the formation of the triiodide ion that is soluble in water. The traditional (100%) Lugol solution has an iodine concentration of 986 mmol/L and has a higher osmolality (1204 mOsm/L) as compared to normal saline (0.9% NaCl, 308 mOsm/L). Thus, 100% Lugol solution was diluted in demineralized water in order to be isotonic to biological tissues and to avoid tissue deformities. Indeed, shrinkage due to water extraction from tissue is possible if samples are immersed in hypertonic solution. Dilution concentrations and time for dilution were chosen according to previous used protocols (53) and sample properties. If $<$ 1.5 g, samples were immersed in 15% dilution Lugol solution. Otherwise, they were immersed in 20% Lugol solution. When thrombus within heart or vessel was present, dilution was reduced to avoid hyper-captation of iodine materials by the blood and consequently final image

degradation. In case of heart-lungs specimens, dimensions instead of weight were used to define correct dilution, with bigger dimensions needing higher Lugol concentration. Immediately before CT, samples were washed with alcohol to remove excess surface iodine and blotted dry. Post-mortem micro-CTs were performed using a micro-CT scanner SkyScan 1176 (Bruker, Kontich, Belgium). Samples were fixed in a polystyrene-made support to avoid movements during acquisition and blurring effect on imaging reconstruction. Raw data were corrected for distortion and detector anomalies, reconstructed by the software NRecon Version, 1.7.4.2 and transformed in DICOM format by the software DicomCT Version 2.5, resulting in a 3D image volume having isotropic resolution. Isotropic voxel size varied between 9 and 18 μm . Acquisition dataset changed for each specimen, according to sample properties and previous described protocol (53). Data were analyzed by a single radiologist with expertise on micro-CT technique and on human fetal heart, who was blinded to prenatal diagnosis. Post-processing analysis was performed using CTVox volume rendering 64 bit version, DATAVIEWER 64 bit version (Bruker, Kontich, Belgium) and Horos v2.4 software (free and open source code software at Horosproject.org). Post processing revisions involved gray value windowing, technique to remove supporting materials and multiplanar reconstruction to create virtual dissection of the fetal hearts. Segmental approach (82) was applied to study the heart.

Autopsy examination

Conventional autopsies were performed by a single senior pediatric cardiac surgeon who was blinded to prenatal findings and micro-CT data. Neonatal surgical instruments and 3.5 magnification loops were used. A standard technique to dissect the heart was adopted (83). It consisted in external evaluation of the heart to define atrial appendage, ventricular shape, form of the apex, presence of great arteries. Section of the sample started from right atrial cavity at the level of inferior and superior vena cava (to define morphological features of the right atria and presence and patency of right atrioventricular valve) and moved to right ventricular inflow and outflow (to define anatomical characteristic of right ventricle and right ventricular outflow tract, presence and patency of pulmonary valve, continuity between right ventricle and pulmonary trunk and its bifurcation). Left heart structures were analyzed as right ones. Segmental approach (82) was applied to study the heart. After macroscopic dissection, hearts were sampled for histological and cytogenetic investigation.

Data analysis

In CHD, cardiac chambers and vessels can be anywhere. This means that their identification cannot be based on their relative position (right or left-sided) or function (venous or arterial, pulmonary or systemic) but rather on their anatomic features. Indeed, morphologic anatomic identification is the cornerstone of accurate diagnosis. Table 1 and 2 summarizes characteristics of right and left atria and ventricles. Definitive cardiac anatomy of CHD is best described dividing the heart in three main segments that are the embryological building blocks of the heart (viscera and atria, ventricles, truncus arteriosus). They are connected by two junctional cardiac segments: the atrioventricular canal, that consists of the

atrioventricular valves and the atrioventricular septum, and the infundibulum or conus arteriosus, that is present in the right ventricle (a muscular cone or funnel beneath the pulmonary valve) and absent in the left ventricle, determining aortic–mitral fibrous continuity). These junctional cardiac segments are interposed between main segments. CHD are described analyzing the main segments, how they are connected through junctional segments and how they are aligned.

Comparison between techniques based only on final diagnosis only superficially analyses ability of the alternative studied technique. Moreover, the comparison would be limited by the high number of samples needed to reach statistical power and the possible ambiguity in differential diagnosis of CHD.

Therefore, we compare techniques according to their ability to define different indices of cardiac anatomy derived from segmental approach (82). Each sample underwent micro-CT and subsequently conventional autopsy. For each case and for each technique, 26 indices of cardiac anatomy were defined and were used to compare techniques (abdominal situs, cardiac position, systemic venous returns, pulmonary venous returns, right and left appendage, coronary sinus, atrial septum, tricuspid valve, mitral valve, ventricular septum, right ventricle, left ventricle, right ventricular outflow tract, left ventricular outflow tract, pulmonary valve, main pulmonary artery, right pulmonary artery, left pulmonary artery, aortic valve, aortic root, atrio-ventricular concordance, ventricular-arterial concordance, aortic arch, arterial duct, other such as coronary arteries). Firstly, each index is defined “visible” or “non-visible”. Secondly, indices are defined “normal”, “abnormal” or “non-diagnostic”. “Non-diagnostic” means that the technique can neither confirm nor deny the normality of that index. Pulmonary venous returns was defined “normal” if at least 2 pulmonary veins were seen terminating in left atrium. We decide to divide “visible” indices in “normal” or “abnormal” and “non-visible” indices in “normal”, “abnormal” or “non-diagnostic” to better investigate diagnostic accuracy. We suppose that the definition of “visible” and “non-visible” indices does not suffice, because it does not mean that CT and autopsy agree in diagnostic conclusion. For example, one index can be considered “visible” by both techniques but it can results “normal” in CT and “abnormal” in autopsy. “Visible” indices represent the sum between “normal” and “abnormal” indices. “Non-visible” indices represent the sum between indices that are “non-diagnostic” in CT but diagnostic in autopsy, “non-diagnostic” in autopsy but diagnostic in CT and “non-diagnostic” by both techniques.

Statistical analysis

The primary outcome is the agreement between micro-CT and conventional autopsy. The secondary outcomes are sensitivity, specificity, PPV and NPV.

We consider firstly conventional autopsy and secondly micro-CT as gold standard technique.

Primary end point is the definition of indices as “visible” or “non-visible”. We define agreement when investigated technique gives the same results as compared to gold standard. It represents the sum between true positive and true negative observations. We define discordance when the investigated technique gives

different results as compared to gold standard. It consists in false positive and false negative observations.

Secondary end point is the definition of indices as “normal”, “abnormal” or “non-diagnostic”. Analysis of agreement relies only on “normal” and “abnormal” indices. We define agreement when investigated technique gives the same results as compared to gold standard. It represents the sum between true positive and true negative observations. We define discordance when the investigated technique gives different results as compared to gold standard. It consists in false positive and false negative observations. Statistical analysis applies to comparable indices. “Non-diagnostic” indices are not comparable and they are only described in the text. For “non-diagnostic” indices, we define “apparent advantage of investigated technique” when the investigated technique would be able to define index as “normal” or “abnormal” while gold standard technique cannot and “apparent advantage of gold standard technique” when gold standard technique is able to define index as “normal” or “abnormal” while investigated technique cannot.

Analysis of primary and secondary end point is made on the whole population and on the subgroup of samples defines “challenging specimens”.

Clinical data (GA at prenatal evaluation, GA at TOP, type of sample, weight of sample, diameters of samples) are summarized by descriptive analysis and expressed as percentage, mean value \pm standard deviation, minimum value, and maximum value.

Agreement, sensitivity, specificity, PPV and NPV are described as percentage, with 95% confidence interval (CI).

RESULTS

Fifty-five cases met the inclusion criteria. One case withdrawn consent and was excluded from the study. In 6 cases, heart was not present or was destroyed and did not undergo further examinations. Micro-CT and conventional autopsy were available for 48 cases. Median GA at prenatal evaluation was 16.3 ± 2.8 weeks (range 12^{+4} - 21^{+4} weeks). Median GA at TOP was 17.0 ± 2.9 weeks (range 12^{+5} - 21^{+6} weeks). CHD were present in 29/48 (60.4 %) cases, of which 7/29 (24.1%) were simple CHD while 22/29 (75.9%) were complex CHD. Twenty-seven out of 29 CHD (93.1%) were associated to chromosomal anomalies or extra-cardiac malformations. Eighteen out of 19 normal hearts (94.7%) were associated to prenatally diagnosed chromosomal anomalies or extra-cardiac malformations. Twenty-four out of 48 (50%) cases belong to the subgroup of “challenging specimen”. In this group, CHD were present in 15/24 (62.5 %) cases, of which 2/15 (13.3%) were simple CHD while 13/15 (86.7%) were complex CHD. Table 3 shows detailed epidemiological data and diagnoses. Micro-CT was conclusive in all cases. Autopsy could not evaluate cardiac structures in 11 out of 48 cases (22.9%), of which 8/11 (72.3%) belong to the subgroup of “challenging specimens”. As compared to conventional autopsy, micro-CT matched the correct diagnosis in 28 out of 37 comparable cases (75.6%). Disagreements between techniques were present in 9 out of 37 comparable cases (24.3%) and mainly regarded position of VSDs and dimension of the great arteries.

Samples were immersed in 10, 15, 20, 25 or 30% Lugol dilution with demineralized water for 48 or 72 hours. Isotropic voxel size varied between 9 to 18 μm . Samples were exposed to 50-90 V with a current range of 264 to 500 μA for a period of 210 to 1150 msec. Table 4 summarizes information on micro-CT setting for proper acquisition.

Samples consisted in heart (31/48, 64.6%) or in heart-lungs (17/48, 35.4%). Mean pre-Lugol weight was 2.66 ± 2.92 g (range 0.13-13.90 g). Mean post Lugol weight was 1.92 ± 2.14 g (range 0.08-10.10 g). Mean longitudinal diameter was 1.38 ± 0.58 cm (range 0.40-3.00 cm). Mean transverse diameter was 1.12 ± 0.45 cm (range 0.40-2.10 cm). SVR and PVR were absent in one sample due to previous cardiac isolation. Great arteries had been torn prior to isolation in 2 cases. In 8 out of 48 cases, autopsy turned out to be impossible because cardiac structures crumbled apart when handled.

Gold standard: autopsy

Primary end point: “visible”/“non-visible” indices

Twenty-six indices were analyzed for each sample and with each technique so that 1248 indices were defined by micro-CT and conventional autopsy and were available for comparison. There was fully agreement for 910 of 1248 indices (73.4%; 95% CI, 71.0-75.8%). This consisted of 596 true positive and 314 true negative indices, giving overall sensitivity of 92.8% (95% CI, 90.9-94.8%) and specificity of 51.8% (95% CI, 48.1-55.5%). PPV and NPV were, respectively, 67.1% (95% CI, 37.6-96.4%) and 87.2% (95% CI, 83.8-90.6%). Specificity identified cases deemed “non-visible” by both techniques. It was generally low because of high number of cases deemed “non-visible” in autopsy and visible in

CT but considered false positive when using autopsy as gold standard. It means that in 48.2% of cases autopsy defined the index as “non-visible” whereas CT would define it as “visible”. PPV express the true visible indices in the group of indices deemed visible by CT. As more indices were defined visible by CT as compared to autopsy and therefore more false positive were present, PPV was generally low. Table 6 describes statistical analysis for each single index. Statistical analysis was not available for abdominal situs and cardiac position because they were never evaluable with autopsy. Except for SVR and PVR, sensitivity was high. It means that CT was able to correctly identify normal indices in the group of true visible indices. Specificity was high for atrial appendage, coronary sinus, aortic and ductal arch, for which both CT and autopsy were not able to define the index. Specificity was generally low for all other indices because they were deemed “visible” by CT and “non-visible” by autopsy and were considered false positive when using autopsy as gold standard.

Secondary end point: “normal”/“abnormal”/“non-diagnostic” indices

26 indices were analyzed for each sample and with each technique. Normal and abnormal indices were 596 while “non-diagnostic” indices were 652. Statistical analysis was made on comparable indices. There was fully agreement for 556 of 596 comparable indices (93.3%; 95% CI, 91.3-95.3%). This consisted of 500 true positive and 56 true negative indices, giving an overall sensitivity of 97.3% (95% CI, 95.9-98.7%) and specificity of 68.3% (95% CI, 58.5-78.1%). PPV and NPV were, respectively, 95.1% (95% CI, 93.3-96.9%) and 80.0% (95% CI, 71-89%). Table 7 describes statistical analysis for each single index. Statistical analysis was not available for abdominal situs and cardiac position because they were never visible with autopsy. Sensitivity was lower for SVR, PVR, branch pulmonary arteries and aortic valve. Specificity and NPV was generally high. PPV value was generally high, except for branch pulmonary arteries.

“Non-diagnostic” indices were 652. In 314 of 652 (48.2%), nor micro-CT nor autopsy were able to define anatomical structures. The remaining 338 indices represented the sum between “apparent advantage of micro-CT” and “apparent advantage of autopsy”. “Apparent advantage of micro-CT” were 291/338 indices (86.1%), of which 267/291 (91.8%) were deemed normal and 24/291 (8.2%) were deemed abnormal by CT. “Apparent advantage of micro-CT” were more numerous for the definition of extra-cardiac structures, especially great arteries, right and left pulmonary arteries, aortic arch and therefore atrio-ventricular and ventriculo-arterial concordance. The last group (“abnormal” at CT/“non-diagnostic” at autopsy) included case 3 (atrial septum), case 5 (aortic valve), case 7 (atrial septum), case 15 (ventricular septum), case 21 (atrial and ventricular septum, mitral and tricuspid valve), case 22 (main and branch pulmonary arteries), case 35 (left ventricle, left and right outflow tract), case 37 (ventricular septum, left ventricular outflow tract, aortic valve, aortic root and arch), case 47 (main and branch pulmonary arteries). “Apparent advantage of autopsy” were 47/338 indices (13.9%), of which 42/47 (89.4%) were deemed normal and 5/47 (10.6%) were deemed abnormal by autopsy. They were more numerous for SVR, PVR and atrial septum. The last group (“non-diagnostic” at CT/“abnormal” at autopsy) referred to case 3 (right and left ventricular outflow tract, pulmonary valve), case 20

(aortic arch) and case 11 (MAPCAs from MPA). Table 8 describes “non-diagnostic” observations, according to each index.

Primary end point: “visible”/“non-visible” indices for the subgroup of challenging specimen

Twenty-six indices were analyzed for each sample and with each technique. 624 indices were defined by microCT and conventional autopsy and were available for comparison. There was fully agreement for 411/624 comparison (65.9%; 95% CI, 62.2-69.6%). This consisted of 232 true positive and 179 true negative indices, giving overall sensitivity of 92.8% (95% CI, 89.7-95.9%) and specificity of 47.8% (95% CI, 43.1-52.5%). PPV and NPV were, respectively, 54.3% (95% CI, 49.6-59%) and 90.9% (95% CI, 87.0-94.8%). Specificity identified cases deemed “non-visible” by both techniques. It was generally low because of high number of cases deemed “non-visible” in autopsy and visible in CT but considered false positive when using autopsy as the gold standard technique. It means that in 52.2% of cases autopsy defined the index as “non-visible” whereas CT would define it as “visible”. PPV stands for true visible indices in the group of indices deemed visible by CT. As more indices were defined visible by CT as compared to autopsy and therefore more false positive were present, PPV was generally low. Table 9 describes statistical analysis for each single index. Statistical analysis was not available for abdominal situs, cardiac position, coronary sinus and ductus arteriosus, because they were never evaluable by autopsy. Statistical analysis for the indices RV, LV, RVOT, LVOT were limited to sensitivity and PPV because micro-CT had only “visible” indices. Except for SVR and PVR, sensitivity was high. It means that CT was able to correctly identify indices in the group of true visible indices. Specificity was high for atrial appendage, aortic arch and other, for which both CT and autopsy were not able to define the index. Specificity was generally low for all other indices that were deemed “visible” by CT and “non-visible” by autopsy and were considered false positive when using autopsy as gold standard.

Secondary end point: “normal”/“abnormal”/“non-diagnostic” indices for the subgroup of challenging specimen

Twenty-six indices were analyzed for each sample and with each technique. Normal and abnormal indices were 232 while “non-diagnostic” indices were 392. Statistical analysis was made on comparable indices. There was fully agreement for 213 of 232 indices (91.8%; 95% CI 88.4-95.2%). This consisted of 179 true positive and 34 true negative indices, giving an overall sensitivity of 95.7% (95% CI 92.8-98.6%) and specificity of 75.6% (95% CI 63.6-87.9%). PPV and NPV were, respectively, 94.2% (95% CI 90.7-97.3%) and 81.0% (95% CI 69.2-92.8%). Table 10 describes statistical analysis for each single index. Statistical analysis was not available for abdominal situs, cardiac position, SVR, PVR, coronary sinus and ductal arch, because they were never visible with autopsy. Sensitivity and specificity were high. PPV and NPV were generally high, except for branch pulmonary arteries which had lower PPV (case 32; both right and left pulmonary arteries were judged abnormal in CT but were normal in autopsy).

“Non-diagnostic” indices were 392. In 179 of 392 (45.7%), nor micro-CT nor autopsy were able to define anatomical structures. The remaining 213 indices represented the sum between “apparent advantage of micro-CT” and “apparent advantage of autopsy”. “Apparent advantage of micro-CT” were 195/213 indices (91.5%), of which 178/195 (91.3%) were deemed normal and 17/195 (8.7%) were deemed abnormal by CT. “Apparent advantage of micro-CT” were more numerous for the definition of the ventricular loop, great arteries, right and left pulmonary arteries, aortic arch and therefore atrio-ventricular and ventriculo-arterial concordance. The last group (“abnormal” at CT/“non-diagnostic” at autopsy) included evaluation of atrial and ventricular septum and atrioventricular valve in case 21, main and branch pulmonary arteries in case 22 and 47, ventricular loop in case 35. “Apparent advantage of autopsy” were 18/213 indices (8.5%), of which 16/18 (88.9%) were deemed normal and 2/18 (11.1%) were deemed abnormal by autopsy. The first group (“non-diagnostic” at CT/“normal” at autopsy) comprised few cases of atrial appendages, interatrial septum and atrioventricular valve. The last one (“non-diagnostic” at CT/“abnormal” at autopsy) referred to aortic arch (1 index; case 20) and other (1 index; case 11; autopsy showed a small orifice in the main pulmonary artery with normal origin of coronary arteries, supposing the presence of major aorto-pulmonary collateral arteries [MAPCAs]). Table 11 describes “non-diagnostic” observations, according to each index.

Gold standard: micro-CT

Primary end point: “visible”/“non-visible” indices

Twenty-six indices were analyzed for each sample and with each technique. 1248 indices were defined by microCT and conventional autopsy and were available for comparison. There was fully agreement for 910 of 1248 indices (73.4%; 95% CI, 71.0-75.8). This consisted of 596 true positive and 314 true negative indices, giving overall sensitivity of 67.1% (95% CI, 37.6-96.4%) and specificity of 87.2% (95% CI, 83.8-90.6%). PPV and NPV were, respectively, 92.8% (95% CI, 90.9-94.8%) and 51.8% (95% CI, 48.1-55.1%). Table 6 describes statistical analysis for each single index. Statistical analysis was not available for abdominal situs and cardiac position because they were never evaluable with CT. Except for specific structures (atrial appendages, atrioventricular valves and ventricles), sensitivity was generally low whereas PPV was generally high. It means that autopsy was able to evaluate few indices but, when feasible, it correctly identified them. Specificity was generally high. NPV was generally low: half of cases defined “non-visible” by autopsy were “visible” in CT (false negative).

Secondary end point: “normal”/“abnormal”/“non-diagnostic” indices

Twenty-six indices were analyzed for each sample and with each technique. Normal and abnormal indices were 596 while “non-diagnostic” indices were 652. Statistical analysis was made on comparable indices. There was fully agreement for 556 of 596 comparable indices (93.3%, 95% CI, 91.3-95.3%). This consisted of 500 true positive and 56 true negative indices, giving an overall sensitivity of 95.1% (95% CI, 93.3-96.9%) and specificity of 80.0% (95% CI, 71-89%). PPV and NPV were, respectively, 68.3% (95% CI, 58.5-78.1%) and 97.2% (95% CI,

95.9-98.7%). Table 7 describes statistical analysis for each single index. Statistical analysis was not available for abdominal situs and cardiac position (because CT was never able to define them) and for SVR, PVR, coronary sinus, right and left appendages, atrioventricular concordance, ductal arch and other (because CT was always able to define them and there were any “abnormal” definition at CT examination). Sensitivity was low for outflow tracts and great arteries. PPV was low for main and branch pulmonary arteries, aortic valve and aortic root. Specificity and NPV were high.

“Non-diagnostic” indices were 652. In 314 of 652 (48.2%), nor micro-CT nor autopsy were able to define anatomical structures. The remaining 338 indices represented the sum between “apparent advantage of autopsy” and “apparent advantage of CT”. “Apparent advantage of autopsy” were 47/338 indices (13.9%), of which 42/47 (89.4%) were deemed normal and 5/47 (10.6%) were deemed abnormal by autopsy. They were mainly related to venous returns, atrial septum and left and right atrial features. Table 8 describes “non-diagnostic” observations, according to each index.

Primary end point: “visible”/“non-visible” indices for the subgroup of challenging specimen

26 indices were analyzed for each sample and with each technique. 624 indices were defined by microCT and conventional autopsy and were available for comparison. There was fully agreement for 411/624 comparison (65.9%; 95% CI, 62.2-69.6%). This consisted of 232 true positive and 179 true negative indices, giving overall sensitivity of 54.3% (95% CI, 49.6-59%) and specificity of 90.9% (95% CI, 87.0-94.8%). PPV and NPV were, respectively, 92.8% (95% CI, 89.7-95.9%) and 47.8% (95% CI, 43.1-52.5%). Table 9 describes statistical analysis for each single index. Statistical analysis was not available for abdominal situs, cardiac position, coronary sinus and ductus arteriosus, because they were never evaluable with autopsy. Sensitivity was generally low but PPV was high. Autopsy could see less than CT, but when it was able to see, it saw correctly. Autopsy could see ventricles, outflow tracts, great arteries and pulmonary branches. Specificity was high. NPV was low: half of cases defined “non-visible” by autopsy were visible in CT (high rate of false negative indices). It concerned all indices, except atrial appendages.

Secondary end point: “normal”/“abnormal”/“non-diagnostic” indices for the subgroup of challenging specimen

Twenty-six indices were analyzed for each sample and with each technique. Normal and abnormal indices were 232 while “non-diagnostic” indices were 392. Statistical analysis is made on comparable indices. There was fully agreement for 213 of 232 indices (91.8%; 95% CI, 88.4-95.2%). This consisted of 179 true positive and 34 true negative indices, giving an overall sensitivity of 94.2% (95% CI, 90.7-97.3%) and specificity of 81.0% (95% CI, 69.2-92.8%). PPV and NPV were, respectively, 95.7% (95% CI, 92.8-98.6%) and 75.6% (95% CI, 63.6-87.9%). Table 10 describes statistical analysis for each single index. Statistical analysis was not available for abdominal situs, cardiac position, coronary sinus,

ductal arch and other because they were never visible with autopsy. All other indices showed high sensitivity, specificity, PPV and NPV.

“Non-diagnostic” indices were 392. In 179 of 392 (45.7%), nor micro-CT nor autopsy were able to define anatomical structures. The remaining 213 indices represented the sum between “apparent advantage of autopsy” and “apparent advantage of CT”. “Apparent advantage of autopsy” consisted in 18/213 indices (8.5%), of which 16/18 (88.9%) were deemed normal and 2/18 (11.1%) were deemed abnormal. The first group (“normal” at autopsy/“non-diagnostic” at CT) comprised few cases of atrial appendages, interatrial septum and atrioventricular valve. The latter one (“abnormal” at autopsy/“non-diagnostic” at CT) referred to aortic arch (1 index; case 20) and other (1 index; case 11; autopsy showed a small orifice in the main pulmonary artery with normal origin of coronary arteries, supposing the presence of MAPCAs). “Apparent advantage of micro-CT” were 195/213 indices (91.5%), of which 178/195 (91.3%) were deemed normal and 17/195 (8.7%) were deemed abnormal. Table 11 describes “non-diagnostic” observations, according to each index.

“Non-diagnostic” indices

“Non-diagnostic” indices were 652 in the global population and 392 in the subgroup of challenging specimens. It means that 60.1% (392/652) of the “non-diagnostic” indices belong to the subgroup of challenging specimen. Table 12 summarizes distribution of “non-diagnostic” indices.

Considering autopsy as gold standard technique, micro-CT would add 23.3% information to diagnosis made by autopsy (291 indices added by CT/1248 total indices). Benefits are higher when considering the subgroup of challenging specimens, where micro-CT would add 31.3% information to diagnosis made by autopsy (195 indices added by micro-CT/624 total indices).

Considering micro-CT as gold standard technique, autopsy would add 3.8% information to micro-CT diagnosis (47 indices added by autopsy/1248 total indices). Advantages are lower when considering the subgroup of challenging specimens, where autopsy would add 2.9% information (18 indices added by autopsy/624 total indices) to micro-CT diagnosis.

Table 13 summarizes critical data of the project.

Figures 1 to 5 represent peculiar examples.

DISCUSSION AND CONCLUSIONS

We demonstrate that micro-CT has adequate diagnostic power as compared to conventional autopsy for definition of human fetal cardiac structures. In about a quarter of cases, conventional autopsy lacks of any diagnostic power whereas micro-CT is able to define cardiac structures. Most of these cases belong to the group of early termination of pregnancy. Micro-CT works correctly for definition of primary end point. Half of indices deemed “non-visible” by autopsy would be visible by CT. Both intra-cardiac anatomy (atrioventricular valves, ventricles and outflow tracts) and extra-cardiac structures (great arteries and pulmonary branches), would benefit from CT scan. Micro-CT shows adequate accuracy for the definition of secondary end point. It is able to correctly classify visible indices as “normal” or “abnormal” in the vast majority of cases. Moreover, it would classify as “normal” or “abnormal” numerous (86.1%) indices deemed “non-diagnostic” at conventional autopsy. In contrast to it, autopsy would add data about normality or abnormality only in 13.9% of indices deemed “non-diagnostic” at CT scan. While advantages of micro-CT regard all indices, benefits from autopsy concern mainly venous returns and atrial structures. Distinctive features of challenging specimens do not reduce diagnostic accuracy of micro-CT for both primary and secondary end points. In the population of “challenging specimens”, micro-CT works correctly for definition of primary end point. Half of indices defined “non-visible” at conventional autopsy would be visible at CT scan. Intra-cardiac anatomy (atrioventricular valves, atrial and ventricular septum), as well as extra-cardiac structures (great arteries and pulmonary branches), would especially benefit from CT scan. Micro-CT shows adequate accuracy for the definition of secondary end point. It correctly classifies visible indices as “normal” or “abnormal” in most cases. Furthermore, 91.5% of “non-diagnostic” indices at autopsy would be defined “normal” or “abnormal” by micro-CT. On the contrary, only 8.5% of “non-diagnostic” indices at micro-CT would be interpreted by autopsy. As in general population, advantages of micro-CT concern all indices while benefits from autopsy regard exclusively venous returns and atrial structures.

Our initial hypotheses are strengthened by the little accuracy for post-mortem evaluation of cardiac structures demonstrated by autopsy, when using CT as gold standard technique. Firstly, high positive predictive value concerns a small number of visible indices. Secondly, low NPV denotes the trend of autopsy to wrongly define “non-visible” indices that are “visible” at CT. Although autopsy is accurate when defining “normal” and “abnormal” indices, it is to be noted that only a small part of indices deemed “non-diagnostic” at CT would be diagnostic at autopsy. Therefore, autopsy does not add significant information to CT examination. When examining autopsy performance, it seems to be more accurate only in evaluating atrial structures.

We try to overcome gaps in evidence of previous published reports by increasing number of observations, considering all possible gestational ages and cardiac conditions and applying sequential analysis to both techniques. To the best of our knowledge, this project represents the largest experience of application of micro-CT in postmortem evaluation of normal and pathological human fetal hearts coming from early and late termination of pregnancy.

As previously described, some anatomic features are peculiar in first trimester (39,72). In the subgroup of “challenging specimens”, we faced with frequent autopsy findings of right or left isomerism in the absence of prenatal suspicion of heterotaxy syndrome and of CT anomalies for the same structures. We suspect that these transient aspects can play a role in the discrepancy we noticed. Conventional autopsy could mistake normal developing features for anomalous aspect while the more accurate micro-CT could be able to correctly identify specific traits (i.e. pectinate muscle) that permit the definition of normal left or right atrial appendage.

Limitations of micro-CT exist. Firstly, micro-CT is feasible only for postmortem cardiac examination due to possible fetal teratogenic effects of ionizing radiation if used in vivo. Secondly, samples can be extremely fragile and difficult to be prepared. Vascular structure can be torn prior to isolation in up to 20-30% of samples. Isolation can damage small cardiac and extra-cardiac structures that are important for diagnosis. Nonetheless, we chose to isolate the heart because absence of extra-cardiac structures allows us to choose appropriate machine settings and to use more specific protocols of iodine staining, as other organs collect iodine solution and can create artifact on reconstructed CT images. Moreover, blood clot should be washed out from heart when preparing the specimen in order to reduce inopportune contrast accumulation. Lastly, technical aspects can be challenging when performing micro-CT, ideally limiting its routine application and restricting its execution and interpretation to trained physician with expertise in the technique and in congenital heart disease. Despite these limitations, as compared to other post-mortem imaging techniques such as high field (9.4T) cMRI and ultrasound, CT showed higher resolution power and lower acquisition time.

To conclude, we think that postmortem micro-CT represents a valid alternative to conventional autopsy for postmortem evaluation of human fetal heart coming from both early and late terminations of pregnancy. Moreover, it bridges the gap of conventional autopsy for the evaluation of very small hearts and meets the clinical need of having a confirmation of first trimester prenatal fetal investigation after early termination of pregnancy or fetal demise.

REFERENCES

1. Hoffman JIE Incidence of congenital heart disease: II. Prenatal incidence *Pediatr Cardiol* (1995);16:155-65 DOI:10.1007/BF00794186
2. Hoffman JIE, Kaplan S The incidence of congenital heart disease. *J Am Coll Cardiol* (2002);39:1890–900 DOI:10.1016/s0735-1097(02)01886-7
3. Bregman S, Frishman WH Impact of Improved Survival in Congenital Heart Disease on Incidence of Disease. *Cardiol Rev.* (2018);2:82-85 doi:10.1097/CRD.0000000000000178
4. Khairy P, Clair M, Fernandes SM, Blume ED, Powell AJ, Newburger JW, Landzberg MJ, Mayer JE Jr Cardiovascular outcomes after the arterial switch operation for D-transposition of the great arteries. *Circulation.* (2013);127:331-9 doi:10.1161/CIRCULATIONAHA.112.135046
5. Owen AR, Gatzoulis MA Tetralogy of Fallot: Late outcome after repair and surgical implications. *Semin Thorac Cardiovasc Surg Pediatr Card Surg Annu* (2000);3:216-226 DOI:10.1053/tc.2000.6038
6. Alexiou C, Mahmoud H, Al-Khaddour A, Gnanapragasam J, Salmon AP, Keeton BR et al Outcome after repair of tetralogy of Fallot in the first year of life. *Ann Thorac Surg* (2001);71:494-500 DOI:10.1016/s0003-4975(00)02444-9
7. Rychik J, Atz AM, Celermajer DS, Deal BJ, Gatzoulis MA, Gewillig MH et al Evaluation and Management of the Child and Adult With Fontan Circulation: A Scientific Statement From the American Heart Association. *Circulation* (2019);139:00–00 DOI:10.1161/CIR.0000000000000696
8. Kverneland LS, Kramer P, Ovroutski S Five decades of the Fontan operation: A systematic review of international reports on outcomes after univentricular palliation. *Congenit Heart Dis.* (2018);2:181-193 doi:10.1111/chd.12570
9. Dolk H, Loane M, Garne E and a European Surveillance of Congenital Anomalies (EUROCAT) Working Group Congenital Heart Defects in Europe. Prevalence and Perinatal Mortality, 2000 to 2005. *Circulation* (2011);123:841-849 doi:10.1161/CIRCULATIONAHA.110.958405
10. Donofrio MT, Moon-Grady AJ, Hornberger LK, Copel JA, Sklansky MS, Abuhamad A et al. American Heart Association Adults With Congenital Heart Disease Joint Committee of the Council on Cardiovascular Disease in the Young and Council on Clinical Cardiology, Council on Cardiovascular Surgery and Anesthesia, and Council on Cardiovascular and Stroke Nursing. Diagnosis and treatment of fetal cardiac disease: a scientific statement from the American Heart

- Association. *Circulation* (2014);129:2183-2242
doi:10.1161/01.cir.0000437597.44550.5d
11. Bonnet D, Coltri A, Butera G, Fermont L, Le Bidois J, Kachaner J, Sidi D.: Detection of Transposition of the Great Arteries in Fetuses Reduces Neonatal Morbidity and Mortality. *Circulation* (1999);99:916-918
DOI:10.1161/01.cir.99.7.916
 12. Tworetzky W, McElhinney D. B, Reddy V. M, Brook M.M, Hanley F.L, Silverman N.H Improved Surgical Outcome After Fetal Diagnosis of Hypoplastic Left Heart Syndrome. *Circulation*. (2001);103:1269-1273
DOI:10.1161/01.cir.103.9.1269
 13. Eapen RS, Rowland DG, Franklin WH. Effect of prenatal diagnosis of critical left heart obstruction on perinatal morbidity and mortality. *Am J Perinatol* (1998);15:237–242 DOI:10.1055/s-2007-993934
 14. Franklin O, Burch M, Manning N, Sleemann K, Gould S, Archer N. Prenatal diagnosis of coarctation of the aorta improves survival and reduces morbidity. *Heart* (2002);87 67–69 DOI:10.1136/heart.87.1.67
 15. Holland B. J, Myers J. A, Woods C. R. Jr Prenatal diagnosis of critical congenital heart disease reduces risk of death from cardiovascular compromise prior to planned neonatal cardiac surgery: a meta-analysis. *Ultrasound Obstet Gynecol* (2015);45:631–638 doi:10.1002/uog.14882
 16. Escobar-Diaz M.C, Freud L.R, Bueno A, Brown D.W, Friedman K.G, Schidlow D, Emani S, Del Nido P.J, Tworetzky W Prenatal diagnosis of transposition of the great arteries over a 20-year period: improved but imperfect. *Ultrasound Obstet Gynecol* (2015);45:678–682 doi:10.1002/uog.14751
 17. Mahle WT, Clancy RR, McGaurn SP, Goin JE, Clark BJ Impact of prenatal diagnosis on survival and early neurologic morbidity in neonates with the hypoplastic left heart syndrome. *Pediatrics*. (2001);107:1277-82
DOI:10.1542/peds.107.6.1277
 18. Gupta N, Leven L, Stewart M, Cheung M, Patel N Transport of infants with congenital heart disease: benefits of antenatal diagnosis. *Eur J Pediatr* (2014) 173:655–660 doi:10.1007/s00431-013-2231-0
 19. Evans W, Castillo W, Rollins R, Luna C, Kip K, Ludwick J et al Moving towards universal prenatal detection of critical congenital heart disease in southern Nevada: a community-wide program. *Pediatr Cardiol*. (2015);36:281-8
doi:10.1007/s00246-014-0996-1

20. Sekar P, Heydarian H, Cnota J, Hornberger L, Michelfelder E Diagnosis of congenital heart disease in an era of universal prenatal ultrasound screening in southwest Ohio. *Cardiol Young.* (2015);25:35-41
21. Van Velzen C, Clur S, Rijlaarsdam M, Bax C, Pajkrt, Heymans M et al Prenatal detection of congenital heart disease--results of a national screening programme. *BJOG.* (2016);123:400-7 doi: 10.1111/1471-0528.13274
22. Hartge DR, Weichert J, Krapp M, Germer U, Gembruch U, Axt-Fliedner R Results of early foetal echocardiography and cumulative detection rate of congenital heart disease. *Cardiol Young.* (2011);21:505-17 doi: 10.1017/S1047951111000345
23. Jegatheeswaran A, Oliveira C, Batsos C, Moon-Grady AJ, Silverman NH, Hornberger LK et al Costs of prenatal detection of congenital heart disease *Am J Cardiol.* (2011);108:1808-14 doi: 10.1016/j.amjcard.2011.07.052
24. EUROCAT www.eurocat-network.eu
25. Yagel S, Silverman NH, Gembruch U Fetal cardiology. embryology, genetics, physiology, echocardiographic evaluation, diagnosis and perinatal management of cardiac diseases. 2009, 2nd ed., Informa Healthcare USA, New York; ISBN-13: 978-0415432658
26. Christoffels VM, Burch JB, Moorman AF Architectural plan for the heart: early patterning and delineation of the chambers and the nodes. *Trends Cardiovasc Med.* (2004);8:301-7 DOI: 10.1016/j.tcm.2004.09.002
27. Stock UA, Vacanti JP Cardiovascular physiology during fetal development and implications for tissue engineering. *Tissue Eng.* (2001);1:1-7 DOI: 10.1089/107632701300003241
28. Rizzo G, Calì G, on behalf of the “Società Italiana di Ecografia Ostetrico Ginecologica e Metodologie Biofisiche”. *Linee guida SIEOG edizione 2015.* Italy: EDITEAM Gruppo Editoriale (2015). Italian
29. Sonek J. First Trimester Ultrasonography in Screening and Detection of Fetal Anomalies. *Am J Med Genet C Semin Med Genet* (2007);145C:45-61 doi: 10.1002/ajmg.c.30120
30. Nicolaides KH, Azar G, Byrne D, Mansur C, Marks K Fetal nuchal translucency: Ultrasound screening for chromosomal defects in first trimester of pregnancy. *BMJ (Clinical Research Ed.)* (1992);304:867–869 DOI: 10.1136/bmj.304.6831.867

31. Hyett J, Moscoso G, Papapanagiotou G, Perdu M, Nicolaides KH Abnormalities of the heart and great arteries in chromosomally normal fetuses with increased nuchal translucency thickness at 11-13 weeks of gestation. *Ultrasound Obstet Gynecol.* (1996);7:245-50 DOI: 10.1046/j.1469-0705.1996.07040245.x
32. Hyett J, Perdu M, Sharland G, Snijders R, Nicolaides KH. Using fetal nuchal translucency to screen for major congenital cardiac defects at 1014 weeks of gestation: population based cohort study. *BMJ* (1999);318:81-85 DOI: 10.1136/bmj.318.7176.81
33. Ghi T, Huggon IC, Zosmer N, Nicolaides KH. Incidence of major structural cardiac defects associated with increased nuchal translucency but normal karyotype. *Ultrasound Obstet Gynecol* (2001);18:610-614 doi: 10.1046/j.0960-7692.2001.00584.x DOI: 10.1046/j.0960-7692.2001.00584.x
34. Sotiriadis A, Papatheodorou S, Eleftheriades M, Makrydimas G Nuchal translucency and major congenital heart defects in fetuses with normal karyotype: a meta-analysis. *Ultrasound Obstet Gynecol.* (2013);42:383-9 doi: 10.1002/uog.12488
35. Nicolaides KH. Screening for fetal aneuploidies at 11 to 13 weeks. *Prenat Diagn* (2011);31:7–15 doi: 10.1002/pd.2637
36. Jakobsen TR, Sogaard K, Tabor A. Implications of a first trimester Down syndrome screening program on timing of malformation detection. *Acta Obstet Gynecol Scand* (2011);90:728–736 doi: 10.1111/j.1600-0412.2011.01156.x
37. Smrcek JM, Berg C, Geipel A, Fimmers R, Diedrich K, Gembruch U Early fetal echocardiography: heart biometry and visualization of cardiac structures between 10 and 15 weeks' gestation. *J Ultrasound Med.* (2006);25:173-82 DOI: 10.7863/jum.2006.25.2.173
38. Fetal echocardiography at 11-13 weeks by transabdominal high-frequency ultrasound. Persico N, Moratalla J, Lombardi CM, Zidere V, Allan L, Nicolaides KH. *Ultrasound Obstet Gynecol.* (2011);37:296-301 doi: 10.1002/uog.8934
39. Hutchinson D, McBrien A, Howley L, Yamamoto Y, Sekar P, Motan T et al. First-Trimester Fetal Echocardiography: Identification of Cardiac Structures for Screening from 6 to 13 Weeks' Gestational Age. *J Am Soc Echocardiogr.* (2017);30:763-772 doi: 10.1016/j.echo.2017.03.017
40. McBrien A, Hornberger LK Early fetal echocardiography. *Birth Defects Res.* (2019);111:370-379 doi: 10.1002/bdr2.1414

41. Gottschalk I, Jehle C, Herberg U, Breuer J, Brockmeier K, Bennink G, Hellmund A, Strizek B, Gembruch U, Geipel A, Berg C Prenatal diagnosis of absent pulmonary valve syndrome from first trimester onwards: novel insights into pathophysiology, associated conditions and outcome. *Ultrasound Obstet Gynecol.* (2017);49:637-642 doi: 10.1002/uog.15977
42. Yu R, Li SL, Luo GY, Wen HX, Ouyang SY, Chen CY, Yuan Y First-Trimester Echocardiographic Features and Perinatal Outcomes in Fetuses With Congenital Absence of the Aortic Valve. *J Ultrasound Med.* (2016);35:739-45 doi: 10.7863/ultra.15.03042
43. Cannie M, Votino C, Moerman Ph, Vanheste R, Segers V, Van Berkel K, Hanssens M, Kang X, Cos T, Kir M, Balepa L, Divano L, Foulon W, De Mey J, Jani J Acceptance, reliability and confidence of diagnosis of fetal and neonatal virtuopsy compared with conventional autopsy: a prospective study. *Ultrasound Obstet Gynecol* (2012); 39:659–665 doi: 10.1002/uog.10079
44. Sinard J. Factors affecting autopsy rates, autopsy request rates, and autopsy findings at a large academic medical center. *Experimental and Molecular Pathology* (2001);70:333–343 doi: 10.1006/exmp.2001.2371
45. Rossi AC, Prefumo F. Correlation between fetal autopsy and prenatal diagnosis by ultrasound: A systematic review. *Eur J Obstet Gynecol Reprod Biol* (2016);210:201-206 doi: 10.1016/j.ejogrb.2016.12.024
46. Carvalho JS, Moscoso G, Tekay A, Campbell S, Thilaganathan B, Shinebourne EA. Clinical impact of first and early second trimester fetal echocardiography on high risk pregnancies. *Heart* (2004);90:921-926 doi: 10.1136/hrt.2003.015065
47. Dickinson JE, Prime DK, Charles AK. The role of autopsy following pregnancy termination for fetal abnormality. *Aust N Z J Obstet Gynaecol* (2007);47:445-449 doi: 10.1111/j.1479-828X.2007.00777.x
48. Taylor AM, Arthurs OJ, Sebire NJ. Postmortem cardiac imaging in fetuses and children. *Pediatr Radiol* (2015);45:549-555 doi: 10.1007/s00247-014-3164-0
49. Liu X, Tobita K, Francis RJB, Lo CW Imaging Techniques for Visualizing and Phenotyping Congenital Heart Defects in Murine Models. *Birth Defects Res C Embryo Today* (2013);99: 93–105 doi:10.1002/bdrc.21037
50. Gregg CL, Butcher JT Translational Paradigms in Scientific and Clinical Imaging of Cardiac Development. *Birth Defects Res C Embryo Today* (2013);99:106–120 doi: 10.1002/bdrc.21034

51. Ritman EL Current Status of Developments and Applications of Micro-CT. *Annu. Rev. Biomed. Eng.* (2011);13:531–52 doi: 10.1146/annurev-bioeng-071910-124717
52. Hutchinson JC, Shelmerdine SC, Simcock IC, Sebire NJ, Arthurs OJ Early clinical applications for imaging at microscopic detail: microfocus computed tomography (micro-CT). *Br J Radiol* (2017);90:20170113. doi: 10.1259/bjr.20170113
53. Degenhardt K, Wright AC, Horng D, Padmanabhan A, Epstein JA. Rapid 3D phenotyping of cardiovascular development in mouse embryos by micro-CT with iodine staining. *Circ Cardiovasc Imaging* (2010) 3:314–322 doi: 10.1161/CIRCIMAGING.109.918482
54. Metscher BD MicroCT for comparative morphology: simple staining methods allow high-contrast 3D imaging of diverse non-mineralized animal tissues. *BMC Physiol* (2009);9:11 doi: 10.1186/1472-6793-9-11
55. Schambach SJ, Bag S, Schilling L, Groden C, Brockmann MA Application of micro-CT in small animal imaging. *Methods* (2010);50:2–13 doi: 10.1016/j.ymeth.2009.08.007
56. Degenhardt K, Wright AC, Horng D, Padmanabhan A, Epstein JA Rapid 3D phenotyping of cardiovascular development in mouse embryos by micro-CT with iodine staining. *Circ Cardiovasc Imaging* (2010);3:314–322 doi: 10.1161/CIRCIMAGING.109.918482
57. Metscher B.D. MicroCT for Developmental Biology: A Versatile Tool for High-Contrast 3D Imaging at Histological Resolutions. *Developmental Dynamics* (2009);238:632–640 doi: 10.1002/dvdy.21857
58. Kim AJ, Francis R, Liu X, Devine WA, Ramirez R, Anderton SJ, Wong LY, Faruque F, Gabriel GC, Chung W, Leatherbury L, Tobita K, Lo CW Microcomputed tomography provides high accuracy congenital heart disease diagnosis in neonatal and fetal mice. *Circ Cardiovasc Imaging* (2013);6:551-9 doi: 10.1161/CIRCIMAGING.113.000279
59. Lombardi CM, Zambelli V, Botta G, Moltrasio F, Cattoretti G, Lucchini V et al. Postmortem microcomputed tomography (micro-CT) of small fetuses and hearts. *Ultrasound Obstet Gynecol* (2014);44:600-609 doi: 10.1002/uog.13330
60. Hutchinson JC, Arthurs OJ, Ashworth MT, Ramsey AT, Mifsud W, Lombardi CM et al. Clinical utility of postmortem microcomputed tomography of the fetal

- heart: diagnostic imaging vs macroscopic dissection. *Ultrasound Obstet Gynecol* (2016);47:58-64 doi: 10.1002/uog.15764
61. Sandrini C, Rossetti L, Zambelli V, Zanarotti R, Bettinazzi F, Soldá R et al Accuracy of Micro-Computed Tomography in Post-mortem Evaluation of Fetal Congenital Heart Disease. Comparison Between Post-mortem Micro-CT and Conventional Autopsy. *Front Pediatr.* (2019);7:92 doi: 10.3389/fped.2019.00092
 62. Jinnouchi H, Torii S, Kutyna M, Sakamoto A, Kolodgie FD, Finn AV, Virmani R Micro-Computed Tomography Demonstration of Multiple Plaque Ruptures in a Single Individual Presenting With Sudden Cardiac Death. *Circ Cardiovasc Imaging.* (2018);10:e008331 doi: 10.1161/CIRCIMAGING.118.008331
 63. Hutchinson JC; Kang X, Shelmerdine SC, Segers V, Lombardi CL, Cannie MM et al Postmortem microfocus computed tomography for early gestation fetuses: a validation study against conventional autopsy. *Am J Obstet Gynecol* (2018);218:445.e1-12 doi: 10.1016/j.ajog.2018.01.040
 64. Thayyil S, Sebire NJ, Chitty LS, Wade A, Chong WK, Olsen O et al for the MARIAS collaborative group Post-mortem MRI versus conventional autopsy in fetuses and children: a prospective validation study. *Lancet* (2013);382,223-33 doi: 10.1016/S0140-6736(13)60134-8
 65. Jawad N, Sebire NJ, Wade A, Taylor AM, Chitty LS, Arthurs OJ Body weight lower limits of fetal postmortem MRI at 1.5T. *Ultrasound Obstet Gynecol* (2016);48: 92–97 doi: 10.1002/uog.14948
 66. Thayyil S, Cleary JO, Sebire NJ, Scott RJ, Chong K, Gunny R et al Post-mortem examination of human fetuses: a comparison of whole-body high-field MRI at 9.4 T with conventional MRI and invasive autopsy. *Lancet.* (2009);374:467-75 doi: 10.1016/S0140-6736(09)60913-2
 67. Votino C, Jani J, Verhoye M, Bessieres B, Fierens Y, Segers V et al Postmortem examination of human fetal hearts at or below 20 weeks' gestation: a comparison of high-field MRI at 9.4 T with lower-field MRI magnets and stereomicroscopic autopsy. *Ultrasound Obstet Gynecol.* (2012);40:437-44 doi: 10.1002/uog.11191
 68. Sandaite I, Dymarkowski S, De Catte L, Moerman P, Gewillig M, Fedele L et al Fetal heart pathology on postmortem 3-T magnetic resonance imaging. *Prenat Diagn.* (2014);34:223-9 doi: 10.1002/pd.4283
 69. Taylor AM, Sebire NJ, Ashworth MT, Schievano S, Scott RJ, Wade A et al Magnetic Resonance Imaging Autopsy Study Collaborative Group Postmortem cardiovascular magnetic resonance imaging in fetuses and children: a masked

- comparison study with conventional autopsy. *Circulation*. (2014);129:1937-44 doi: 10.1161/CIRCULATIONAHA.113.005641
70. Pervolaraki E, Anderson RA, Benson AP, Hayes-Gill B, Holden AV, Moore BJ, Paley MN, Zhang H Antenatal architecture and activity of the human heart. *Interface Focus*. (2013);3:20120065 doi: 10.1098/rsfs.2012.0065
 71. Votino C, Cannie M, Segers V, Dobrescu O, Dessy H, Gallo V et al Virtual autopsy by computed tomographic angiography of the fetal heart: a feasibility study. *Ultrasound Obstet Gynecol* (2012);39:679–684 doi: 10.1002/uog.11150
 72. Matsui H, Mohun T, Gardiner HM Three-dimensional reconstruction imaging of the human foetal heart in the first trimester. *Eur Heart J*. (2010);31:415 doi:10.1093/eurheartj/ehp511
 73. Gindes L, Matsui H, Achiron R, Mohun T, Ho Sy, Gardiner H Comparison of ex-vivo high-resolution episcopic microscopy with in-vivo four-dimensional high-resolution transvaginal sonography of the first-trimester fetal heart. *Ultrasound Obstet Gynecol* (2012);39:196–202 doi: 10.1002/uog.9068
 74. Matsui H, Ho SY, Mohun TJ, Gardiner HM Postmortem high-resolution episcopic microscopy (HREM) of small human fetal hearts. *Ultrasound Obstet Gynecol* (2015);45:492–493 doi: 10.1002/uog.14812
 75. Gonzalez-Tendero A, Zhang C, Balicevic V, Cárdenes R, Loncaric S, Butakoff C, Paun B et al Whole heart detailed and quantitative anatomy, myofibre structure and vasculature from X-ray phase-contrast synchrotron radiation-based micro computed tomography. *Eur Heart J Cardiovasc Imaging*. (2017);18:732-741 doi: 10.1093/ehjci/jew314
 76. Dejea H, Garcia-Canadilla P, Cook AC, Guasch E, Zamora M, Crispi F et al Comprehensive Analysis of Animal Models of Cardiovascular Disease using Multiscale X-Ray Phase Contrast Tomography. *Sci Rep*. (2019);9:6996 doi: 10.1038/s41598-019-43407-z
 77. López-Guimet J, Peña-Pérez L, Bradley RS, García-Canadilla P, Disney C, Geng H et al MicroCT imaging reveals differential 3D micro-scale remodelling of the murine aorta in ageing and Marfan syndrome. *Theranostics*. (2018);8:6038-6052 doi: 10.7150/thno.26598
 78. Garcia-Canadilla P, Dejea H, Bonnin A, Balicevic V, Loncaric S, Zhang C et al Complex Congenital Heart Disease Associated With Disordered Myocardial Architecture in a Midtrimester Human Fetus. *Circ Cardiovasc Imaging*. (2018);11:e007753 doi: 10.1161/CIRCIMAGING.118.007753

79. Kaneko Y, Shinohara G, Hoshino M, Morishita H, Morita K, Oshima Y et al Intact Imaging of Human Heart Structure Using X-ray Phase-Contrast Tomography. *Pediatr Cardiol.* (2017);38:390-393 doi: 10.1007/s00246-016-1527-z
80. Votino C, Cos Sanchez T, Bessieres B, Segers V, Kadhim H, Razavi F, Condorelli M, Votino R, D'ambrosio V, Jani J Minimally invasive fetal autopsy using ultrasound: a feasibility study. *Ultrasound Obstet Gynecol* (2018);52:776–783 doi 10.1002/uog.14642
81. Human Tissue Act 2004. <https://www.hta.gov.uk/codes-practice>.
82. Keane JF, Fyler DC, Lock JE. Segmental Approach to Diagnosis. In: Saunders editor. *Nadas' Pediatric Cardiology*. US: Elsevier, 2006: 39-46
83. Basso C, Aguilera B, Banner J, Cohle S, d'Amati G, de Gouveia RH Guidelines for autopsy investigation of sudden cardiac death: 2017 update from the Association for European Cardiovascular Pathology. *Virchows Arch.* (2017);471:691-705 doi: 10.1007/s00428-017-2221-0

TABLES

Table 1: morphologic anatomic features of right and left atrium

ANATOMIC FEATURES	RIGHT ATRIUM	LEFT ATRIUM
VEINS	IVC, constant	Pulmonary veins, variable
SVC, variable		
CS, variable		
APPENDAGE	Broad, triangular	Narrow, finger-like
MUSCULI PECTINATI	Many	Few
CRISTA TERMINALIS	Present	Absent
TINEA SAGITTALIS	Present	Absent
SEPTAL SURFACE	Septum secundum	Septum primum
CONDUCTION SYSTEM	Sino-atrial node	None

IVC: inferior vena cava; SVC: superior vena cava; CS: coronary sinus

Table 2: morphologic anatomic features of right and left ventricle

ANATOMIC FEATURES	RIGHT VENTRICLE	LEFT VENTRICLE
TRABECOLAE CARNAE	Coarse, few, straight	Fine, numerous, oblique
PAPILLARY MUSCLE	Numerous, small, attaching to septal and free wall	Two, large, free wall origins only
ATRIOVENTRICULAR VALVE LEAFLETS	Three, approximately equal depth	Two, very unequal depth
INFUNDIBULUM	Well developed	Absent
SEMI-LUNAR AV FIBROUS CONTINUITY	Absent	Present
CORONARIES	One	Two
CONDUCTION SYSTEM RADIOATIONS	One	Two

Table 3: epidemiologic data

CASE	GA AT PRENATAL EVALUATION (week)	INDICATION FOR PRENATAL EVALUATION	TYPE OF CHD AT PRENATAL EVALUATION (IF ANY)	TYPE OF EXTRA-CARDIAC OR CHROMOSOMAL ANOMALIES (IF ANY)	GA AT TOP	AGREE BETWEEN CT AND AUTOPSY (Y yes, N no)	MICRO-CT DIAGNOSIS	AUTOPSY DIAGNOSIS
1	20 ⁺⁰	extra-cardiac anomaly, suspected CHD	posterior malalignment VSD, aortic hypoplasia	VACTERL; normal karyotype	20 ⁺⁴	Y	borderline LV, mild aortic hypoplasia	borderline LV, mild aortic hypoplasia
2	16 ⁺²	suspected CHD	TOF	frontal bossing, hands anomaly; normal karyotype	18 ⁺⁶	Y	TOF	TOF
3	20 ⁺²	extra-cardiac anomaly, suspected CHD	large VSD, large ASD, small LV and aorta	Bilateral palatine cleft, bilateral renal ptosis, bilateral superior syndactyly, artrogriposis; 46,XY,del(11)(q23.3) (Jacobsen syndrome)	20 ⁺⁴	Y	PA-VSD/truncus	PA-VSD/truncus
4	16 ⁺¹	chromosomal anomaly	VSD	trisomy 21	16 ⁺⁵	y	normal	normal
5	21 ⁺²	suspected CHD	HLHS	/	21 ⁺⁶	Y	HLHS	HLHS
6	16 ⁺²	extra-cardiac anomaly, chromosomal anomaly, suspected CHD	PA-VSD/truncus arteriosus	IUGR, hydrocephaly, posterior fossa anomaly, absence nasal bone; Trisomy 9	16 ⁺³	Y	PA-VSD	PA-VSD
7	12 ⁺⁴	Increased NT (4.7 mm)	AVSD	Trisomy 21	13 ⁺⁶	Y	AVSD	AVSD
8	14 ⁺³	chromosomal anomaly	AVSD	Trisomy 21	14 ⁺³	Y	VSD inlet type	VSD inlet type
9	17 ⁺²	extra-cardiac anomaly, suspected CHD	TOF	Omphalocele	18 ⁺²	Y	VSD TOF type	VSD TOF type
10	13 ⁺²	chromosomal anomaly	AVSD	Trisomy 21	13 ⁺⁴	Y	AVSD	AVSD
11	14 ⁺⁰	suspected CHD	dextrocardia, conoventricular VSD, side by side great arteries probably emerging from RV	cerebellar anomaly, bilateral renal pielectasia, hypertelorism; trisomy X	17 ⁺¹	N	Possible dextrocardia (boot-shaped apex), VSD inlet type	conoventricular VDS
12	17 ⁺⁴	extra-cardiac anomaly	/	fetal hydrops; normal karyotype	17 ⁺⁵	Y	normal	normal
13	13 ⁺³	suspected CHD	/	/	16 ⁺⁰	N	Muscular VSD	normal
14	12 ⁺⁶	extra-cardiac anomaly	unbalanced AVSD, aortic hypoplasia	omphalocele, small bladder, hands anomaly	12 ⁺⁶	not evaluable	any heart in the sample	any heart in the sample
15	12 ⁺⁵	chromosomal anomaly	AVSD	trisomy 21	12 ⁺⁵	N	AVSD, possible TOF	not evaluable
16	12 ⁺⁵	increased NT (4.6 mm)	AVSD	trisomy 21	15 ⁺⁰	N	AVSD	AVSD, possible DORV
17	16 ⁺⁴	suspected CHD	muscular VSD, right aortic arch	trisomy 21	17 ⁺⁵	Y	right aortic arch	right aortic arch
18	12 ⁺⁰	suspected CHD	univentricular heart	fetal hydrops	12 ⁺⁶	not evaluable	any heart in the sample	any heart in the sample
19	12 ⁺⁴	extra-cardiac anomaly	/	acrania	12 ⁺⁶	Y	normal	normal
20	14 ⁺⁶	suspected CHD	AVSD	trisomy 21	14 ⁺⁶	N	AVSD	Mild aortic hypoplasia
21	12 ⁺⁴	chromosomal anomaly	AVSD	trisomy 21	12 ⁺⁶	N	AVSD	not evaluable
22	13 ⁺²	chromosomal anomaly	TOF	trisomy 18	13 ⁺³	N	DORV TOF type	not evaluable
23	21 ⁺⁰	extra-cardiac anomaly	levoposition, inlet VSD	skeletal and vertebral anomalies, feet anomalies, thoracic hypoplasia	21 ⁺³	N	VSD inlet type	conoventricular VSD
24	19 ⁺⁰	suspected CHD	PA-VSD/truncus	dandy walker syndrome	20 ⁺⁰	withdrawn consent	withdrawn consent	withdrawn consent

25	16 ⁺¹	chromosomal anomaly	/	trisomy 21	18 ⁺⁰	Y	normal	normal
26	12 ⁺⁰	increased NT (8 mm)	DORV	Absence nasal bone; trisomy 13	13 ⁺³	not evaluable	any heart in the sample	any heart in the sample
27	14 ⁺⁴	familial history (mutation gene RNF220 NM_018150 causative of leucodistrofin anomaly with cardiac impairment – dilated cardiomyopathy)	/	RNF220 NM_018150 causative of leucodistrofin anomaly with cardiac impairment – dilated cardiomyopathy)	15 ⁺⁰	Y	normal	normal
28	12 ⁺⁴	suspected CHD	HLHS	/	14 ⁺¹	N	univentricular heart, aortic hypoplasia	univentricular heart, pulmonary hypoplasia
29	15 ⁺¹	increased NT (3.4 mm)	/	trisomy 21	19 ⁺⁰	Y	normal	normal
30	21 ⁺⁰	suspected CHD	DORV TOF type	/	21 ⁺⁰	N	normal	VSD, pulmonary hypoplasia
31	19 ⁺⁰	extra-cardiac anomaly	Inlet VSD	dandy walker syndrome	19 ⁺⁰	Y	normal	normal
32	14 ⁺³	suspected CHD	AVSD+TOF	trisomy 21	14 ⁺⁰	Y	AVSD+TOF	AVSD+TOF
33	15 ⁺⁰	chromosomal anomaly	/	trisomy 21	15 ⁺⁰	N	normal	not evaluable
34	19 ⁺²	extra-cardiac anomaly	perimembranous VSD	anencephaly	20 ⁺⁵	N	normal	not evaluable
35	14 ⁺⁰	increased NT (9.4 mm)	DORV with large inlet VSD, small LV	/	14 ⁺⁶	N	DORV, mild hypoplasia of the left ventricle	VSD, one great artery of unknown morphology, left isomerism
36	21 ⁺¹	extra-cardiac anomaly	/	severe renal dysplasia, absence of bladder, anidramnios, CNS anomalies, hands anomaly; lip anomaly	21 ⁺²	N	normal	left isomerism, biventricular hypertrophy
37	16 ⁺¹	suspected CHD	HLHS	polycystic kidney, absence of cerebellum, stomach and bladder	16 ⁺⁴	N	HLHS	univentricular heart (unknown ventricular and arterial morphology), right isomerism
38	14 ⁺³	chromosomal anomaly	inlet VSD	trisomy 21	14 ⁺³	N	normal	Not evaluable
39	11 ⁺¹	extra-cardiac anomaly	AVSD	omphalocele, dilation of bladder, oligoamnios	11 ⁺⁶	not evaluable	any heart in the sample	any heart in the sample
40	15 ⁺⁴	suspected CHD	TA	/	18 ⁺⁴	Y	TA, VSD, transposed great arteries	TA, VSD, transposed great arteries
41	18 ⁺⁰	increased NT (6 mm)	/	fetal hydrops Hands and feet anomaly, frontal bossing; Terminal duplication 4p16.3, terminal deletion 14q32.2q32.33, duplication 14q21.2	21 ⁺⁵	Y	normal (mild biventricular hypertrophy)	normal
42	16 ⁺⁰	extra-cardiac anomaly	/	IUGR, occipital encephalocele, frontal bossing, hands and feet anomaly, renal hyperecogenicity; normal karyotype	16 ⁺⁵	Y	normal	Normal, possible right isomerism
43	18 ⁺⁵	extra-cardiac anomaly	/	acrania	18 ⁺⁵	Y	normal	normal
44	17 ⁺⁵	chromosomal anomaly	/	turner syndrome	18 ⁺⁰	Y	normal	normal
45	13 ⁺⁴	increased NT (5 mm)	/	trisomy 21	14 ⁺⁶	N	normal	not evaluable
46	17 ⁺⁵	extra-cardiac anomaly	/		20 ⁺⁰	N	normal	not evaluable
47	13 ⁺⁰	increased NT (5.5 mm)	/	trisomy 21	14 ⁺⁵	Y	Mild hypoplasia of one great artery (unknown morphology)	Mild hypoplasia of one great artery (unknown morphology), left isomerism

48	14 ⁺¹	chromosomal anomaly	/	trisomy 21	14 ⁺¹	N	normal	not evaluable
49	20 ⁺⁵	extra-cardiac anomaly	/	flat nose, jaw anomaly	21 ⁺³	not evaluable	any heart in the sample	any heart in the sample
50	15 ⁺⁵	increased NT (6.8 mm)	DORV	fetal hydrops; trisomy 21	17 ⁺³	not evaluable	any heart in the sample	any heart in the sample
51	20 ⁺²	suspected CHD	TOF	multiple choroid plexus cysts; trisomy 18	21 ⁺⁴	Y	conovertricular VSD	conovertricular VSD
52	13 ⁺⁰	extra-cardiac anomaly	/	cystic hygroma, hand s anomaly; trisomy 18	14 ⁺⁰	N	normal	not evaluable
53	18 ⁺³	extra-cardiac anomaly	/	renal anomalies, bladder hypoplasia, anidramnios	18 ⁺³	Y	normal	normal
54	21 ⁺⁴	extra-cardiac anomaly	/	vertebral anomaly	21 ⁺⁵	Y	VSD	VSD
55	20 ⁺⁰	extra-cardiac anomaly	right aortic arch	skeletal anomaly	20 ⁺⁰	Y	right aortic arch	right aortic arch

NT: nuchal translucency; VSD: ventricular septal defect, TOF: tetralogy of Fallot, ASD: atrial septal defect; LV: left ventricle; HLHS: hypoplastic left heart syndrome; PA-VSD pulmonary atresia/ventricular septal defect; AVSD: atrioventricular septal defect; RV: right ventricle; TA: tricuspid atresia; CNS: central nervous system; IUGR: intra uterine growth restriction

Table 4: micro-CT settings for acquisition

ID	% LUGOL	h LUGOL	FILTER MICRO-CT	RESOLUTION (μm)	EXPOSITION TIME (msec)	ENERGY RANGE (V)	CURRENT RANGE (μA)	ROTATIONAL STEP (°)
1	25	72	Cu+Al	18	500	89	264	0.50
2	25	72	Cu+Al	18	500	89	264	0.50
3	25	72	Cu+Al	18	500	89	264	0.50
4	20	72	Cu+Al	18	500	89	264	0.50
5	25	72	Cu+Al	18	500	89	264	0.50
6	20	72	Al 0.5mm	18	210	50	500	0.50
7	20	72	Al 0.5mm	9	900	50	500	0.30
8	20	72	Al 0.5mm	18	210	50	500	0.50
9	25	72	Cu+Al	18	500	89	264	0.50
10	20	72	Al 0.5mm	9	900	50	500	0.30
11	20	72	Cu+Al	18	300	80	300	0.70
12	20	72	Cu+Al	18	300	80	300	0.70
13	20	72	Cu+Al	18	300	80	300	0.70
15	15	48	Al 0.5mm	18	210	50	500	0.50
16	30	72	Cu+Al	18	300	80	300	0.70
17	30	72	Cu+Al	18	300	80	300	0.70
19	20	48	Al 0.5mm	18	210	50	500	0.50
20	30	72	Cu+Al	18	300	80	300	0.70
21	15	48	Al 0.5mm	18	210	50	500	0.50
22	30	72	Cu+Al	18	300	80	300	0.70
23	25	72	Cu+Al	18	300	80	300	0.70
25	25	72	Cu+Al	18	300	80	300	0.70
27	20	72	Cu+Al	18	300	80	300	0.70
28	30	72	Cu+Al	18	300	80	300	0.70
29	25	72	Cu+Al	18	300	80	300	0.70
30	20	72	Cu 0.1	18	300	90	270	0.50
31	20	72	Cu 0.1	18	300	90	270	0.50
32	15	48	Cu 0.1	9	1150	90	270	0.50
33	10	24	Cu+Al	9	1050	80	300	0.50
34	25	48	Cu 0.1	18	300	90	270	0.50
35	15	72	Cu+Al	18	300	80	300	0.50
36	25	48	Cu 0.1	18	300	90	270	0.50
37	20	72	Cu+Al	9	1050	80	300	0.50
38	15	48	Cu+Al	18	300	80	300	0.50
40	15	72	Cu+Al	18	300	80	300	0.50
41	20	72	Cu+Al	18	300	80	300	0.50
42	15	72	Cu+Al	18	300	80	300	0.50
43	15	72	Cu+Al	18	300	80	300	0.50
44	20	72	Cu+Al	9	1050	80	300	0.50
45	15	48	Cu+Al	18	300	80	300	0.50
46	15	72	Cu+Al	18	300	80	300	0.50
47	20	72	Cu+Al	18	300	80	300	0.50
48	15	72	Cu+Al	9	1050	80	300	0.50
51	20	72	Cu+Al	18	300	80	300	0.50
52	15	48	Cu+Al	18	300	80	300	0.50
53	20	72	Cu+Al	9	300	80	300	0.50
54	20	72	Cu+Al	9	1050	80	300	0.50
55	20	72	Cu+Al	9	1050	80	300	0.50

Table 5: macroscopic data

ID	SAMPLE	WEIGHT PRE micro- CT (g)	WEIGHT POST micro- CT (g)	LONGITUDINAL DIAMETER (cm)	TRANSVERSE DIAMETER (cm)
1	heart	3.37	2.42	1.50	1.30
2	heart	3.07	2.21	1.50	1.30
3	heart	3.33	2.18	1.50	1.20
4	heart	1.32	0.83	1.00	0.80
5	heart	4.00	3.21	1.70	1.80
6	heart	0.65	0.45	1.10	0.80
7	heart	0.39	0.18	0.60	0.50
8	heart	0.49	0.37	1.00	0.70
9	heart	1.80	1.55	1.40	1.30
10	heart	0.40	0.12	0.50	0.50
11	heart	0.69	0.47	0.80	0.80
12	heart	0.64	0.43	0.90	0.90
13	heart	0.82	0.60	1.00	1.00
15	heart	0.92	0.58	0.40	0.40
16	heart	1.44	1.03	1.20	1.20
17	heart-lungs	0.82	5.60	1.50	1.50
19	heart	0.94	0.59	0.80	0.80
20	heart-lungs	0.82	0.65	1.10	1.10
21	heart	0.88	0.56	n.e.	n.e.
22	heart-lungs	8.27	5.74	n.e.	n.e.
23	heart-lungs	1.25	0.68	1.10	1.00
25	heart	1.58	1.08	2.00	2.00
27	heart	0.51	0.28	1.30	1.30
28	heart-lungs	3.34	1.81	1.40	1.40
29	heart	1.29	0.92	2.00	2.00
30	heart	3.45	1.95	2.40	1.90
31	heart	1.68	0.86	2.00	1.40
32	heart	0.61	0.31	1.20	1.00
33	heart	0.13	0.08	0.80	0.50
34	heart-lungs	13.40	10.10	1.30	1.10
35	heart-lungs	1.33	0.69	1.10	0.90
36	heart-lungs	13.90	9.40	2.80	2.10
37	heart-lungs	5.10	2.99	1.60	1.00
38	heart-lungs	2.90	1.61	1.40	0.90
40	heart	1.20	0.93	1.40	1.00
41	heart	2.27	1.63	2.00	1.00
42	heart-lungs	4.16	3.33	1.20	0.90
43	heart	1.36	0.98	1.50	1.20
44	heart-lungs	7.65	5.05	1.20	1.10
45	heart-lungs	1.70	1.43	1.00	0.80
46	heart	1.26	0.99	1.40	1.10
47	heart-lungs	4.54	2.51	1.10	0.60
48	heart-lungs	2.41	1.18	1.00	0.60
51	heart	2.23	1.52	2.00	1.40
52	heart-lungs	1.00	0.87	0.80	0.50
53	heart-lungs	6.09	3.74	1.80	1.40
54	heart	3.60	2.69	2.20	1.70
55	heart	2.81	1.87	3.00	1.60

n.e.: not evaluable

Table 6: analysis of primary end point for the general population

INDEX	GOLD STANDARD=AUTOPSY				GOLD STANDARD=MICRO-CT			
	SENSITIVITY (%) (95% CI)	SPECIFICITY (%) (95% CI)	PPV (%) (95% CI)	NPV (%) (95% CI)	SENSITIVITY (%) (95% CI)	SPECIFICITY (%) (95% CI)	PPV (%) (95% CI)	NPV (%) (95% CI)
SVR	23.8 (8.2-47.2%)	48.1 (28.7-68.1%)	26.3 (9.15-51.2%)	44.8 (26.4-64.3%)	26.32 (9.2-51.2%)	44.83 (26.4-64.3%)	23.81 (8.22-47.2%)	48.15 (28.7-68.1%)
PVR	20 (0.5-71.6%)	55.8 (39.9-70.9%)	5 (0.1-24.9%)	85.7 (67.3-96.0%)	5.00 (0.1-24.9%)	85.71 (67.3-96%)	20.00 (0.505-71.6%)	55.81 (39.9-70.9%)
RA	93.3 (81.7-98.6%)	0 (0-70.8%)	93.3 (81.7-98.6%)	0 (0-70.8%)	93.33 (81.7-98.6%)	0 (0-70.8%)	93.33 (81.7-98.6%)	0 (0-70.8%)
LA	93.5 (82.1-98.6%)	0 (0-84.2%)	95.6 (84.9-99.5%)	0 (0-70.8%)	96.56 (84.9-99.5%)	0 (0-70.8%)	93.48 (82.1-98.6%)	0 (0-84.2%)
CORONARY SINUS	0 (0-84.2%)	87 (73.7-95.1%)	0 (0-45.9%)	95.2 (83.8-99.4%)	0 (0-45.9%)	95.24 (83.8-99.4%)	0 (0-84.2%)	89.96 (73.7-95.1%)
ATRIAL SEPTUM	83.3 (65.3-94.4%)	22.2 (6.4-47.6%)	64.1 (47.2-78.8%)	44.1 (13.7-78.8%)	64.10 (47.2-78.8%)	44.44 (13.7-78.8%)	83.33 (65.3-94.4%)	22.22 (6.4-47.6%)
TV	92.9 (80.5-98.5%)	33.3 (4.3-77.7%)	90.7 (77.9-97.4%)	40.5 (0.3-85.3%)	90.70 (77.9-97.4%)	40 (5.3-85.3%)	92.86 (80.5-98.5%)	33.33 (4.3-77.7%)
MV	90.2 (76.9-97.3%)	14.3 (0.4-57.9%)	86 (72.1-94.7%)	20 (0.5-71.6%)	86.05 (72.1-94.7%)	20 (0.5-71.6%)	90.24 (76.9-97.3%)	14.29 (0.4-57.9%)
VENTRICULAR SEPTUM	100 (90.3-100%)	33.3 (10.0-65.1%)	81.8 (67.3-91.8%)	100 (39.8-100%)	81.82 (67.3-91.8%)	100 (39.8-100%)	100 (90.3-100%)	33.33 (10.0-65.1%)
RV	100	NC	100	NC	79.17	NC	100	NC
LV	100	NC	100	NC	79.17	NC	100	NC
RVOT	97.2 (85.5-99.9%)	0 (0-26.5%)	74.5 (59.7-86.1%)	0 (0-97.5%)	74.47 (59.7-86.1%)	0 (0-97.5%)	97.22 (85.5-99.9%)	0 (0-26.5%)
LVOT	97 (84.2-99.9%)	0 (0-21.8%)	68.1 (52.9-80.9%)	0 (0-97.5%)	68.09 (52.9-80.9%)	0 (0-97.5%)	96.67 (84.2-99.9%)	0 (0-21.8%)
PV	95.2 (76.2-99.9%)	25.9 (11.1-46.3%)	50 (33.8-66.2%)	87.5 (47.3-99.7%)	50 (33.8-66.2%)	87.50 (47.3-99.7%)	95.24 (76.2-99.9%)	25.93 (11.1-46.3%)
MPA	100 (88.1-100%)	21.1 (6.0-45.6%)	65.9 (50.1-79.5%)	100 (39.8-100%)	65.91 (50.1-79.5%)	100 (39.8-100%)	100 (88.1-100%)	21.05 (6.0-45.6%)
RPA	95.7 (78.1-99.9%)	24 (9.4-45.1%)	53.7 (37.4-69.3%)	85.7 (42.1-99.6%)	53.66 (37.4-69.3%)	85.71 (42.1-99.6%)	100 (78.1-99.9%)	24.00 (9.4-45.1%)
LPA	95.5 (77.2-99.9%)	23.1 (9.0-43.6%)	51.2 (35.1-67.1%)	85.7 (42.1-99.6%)	51.22 (35.1-67.1%)	85.71 (42.1-99.6%)	95.45 (77.2-99.9%)	23.08 (9.0-43.6%)
Ao VALVE	100 (85.2-100%)	28 (12.1-49.4%)	56.1 (39.7-71.5%)	100 (59.0-100%)	56.10 (39.7-71.5%)	100 (59.0-100%)	100 (85.2-100%)	28 (12.1-49.4%)
Ao ROOT	100 (89.7-100%)	21.4 (4.7-50.8%)	75.6 (60.5-87.1%)	100 (29.2-100%)	75.56 (60.5-87.1%)	100 (29.2-100%)	100 (89.7-100%)	21.43 (4.7-50.8%)
AV CONCORDANCE	100 (88.8-100%)	11.8 (1.5-36.4%)	67.4 (52.0-80.5%)	100 (15.8-100%)	67.4 (52.0-80.5%)	100 (15.8-100%)	100 (88.8-100%)	11.76 (1.5-36.4%)
VA CONCORDANCE	100 (89.4-100%)	13.3 (1.7-40.5%)	71.7 (56.5-84%)	100 (15.8-100%)	71.74 (56.5-84%)	100 (15.8-100%)	100 (89.4-100%)	13.33 (1.7-40.5%)
Ao ARCH	90 (55.5-99.7%)	60.5 (43.4-76.0%)	37.5 (18.8-59.4%)	95.8 (78.9-99.9%)	37.50 (18.8-59.4%)	95.83 (78.9-99.9%)	90 (55.5-99.7%)	60.53 (43.4-76%)
DUCTAL ARCH	100 (15.8-100%)	67.4 (52.0-80.5%)	11.8 (1.5-36.4%)	100 (88.8-100%)	11.76 (1.5-36.4%)	100 (88.8-100%)	100 (15.8-100%)	67.39 (52.0-80.5%)

OTHER	100 (2.5-100%)	83 (69.2-92.4%)	11.1 (2.8-48.2%)	100 (91.0-100%)	11.11 (0.3-48.2%)	100 (91.0-100%)	11.11 (2.5-100%)	100 (69.2-92.4%)
--------------	----------------	-----------------	------------------	-----------------	-------------------	-----------------	------------------	------------------

SVR: systemic venous returns; PVR: pulmonary venous returns; RA: right appendage; LA: left appendage; TV: tricuspid valve; MV: mitral valve; RVOT: right ventricular outflow tract; LVOT: left ventricular outflow tract; PV: pulmonary valve; MPA: main pulmonary artery; RPA: right pulmonary artery; LPA: left pulmonary artery; Ao: aortic; AV: atrio-ventricular; VA: ventriculo-arterial; NC: not calculable

Table 7: analysis of secondary end point for the general population

INDEX	GOLD STANDARD=AUTOPSY				GOLD STANDARD=MICRO-CT			
	SENSITIVITY (%) (95% CI)	SPECIFICITY (%) (95% CI)	PPV (%) (95% CI)	NPV (%) (95% CI)	SENSITIVITY (%) (95% CI)	SPECIFICITY (%) (95% CI)	PPV (%) (95% CI)	NPV (%) (95% CI)
SVR	23.8	NC	NC	NC	NC	NC	NC	NC
PVR	20.0	NC	NC	NC	NC	NC	NC	NC
RA	92.9	NC	NC	NC	92.9	NC	NC	NC
LA	93.2	NC	NC	NC	95.3	NC	NC	NC
CORONARY SINUS	0	NC	NC	NC	NC	NC	NC	NC
ATRIAL SEPTUM	75.0 (19.4-99.4%)	100 (83.9-100%)	100 (29.2-100%)	95.5 (77.2-99.9%)	100 (29.2-100%)	95.5 (77.2-99.9%)	75 (19.4-99.4%)	100 (83.9-100%)
TV	71.4 (29.0-96.3%)	100 (89.1-100%)	100 (47.8-100%)	94.1 (80.3-99.3%)	100 (47.8-100%)	94.1 (80.3-99.3%)	71.4 (29.0-96.3%)	100 (89.1-100%)
MV	85.7 (42.1-99.6%)	100 (88.4-100%)	100 (54.1-100%)	96.8 (83.3-99.9%)	100 (54.1-100%)	96.8 (83.3-99.9%)	85.7 (42.1-99.6%)	100 (88.4-100%)
VENTRICULAR SEPTUM	86.7 (59.5-98.3%)	85.7 (63.7-97%)	81.3 (54.4-96%)	90 (68.3-98.8%)	81.3 (54.4-96.0%)	90 (68.3-98.8%)	86.7 (59.5-98.3%)	85.7 (63.7-97.0%)
RV	66.7 (9.4-99.2%)	100 (90-100%)	100 (15.8-100%)	97.2 (85.5-99.9%)	100 (15.8-100%)	97.2 (85.5-99.9%)	66.7 (9.4-99.2%)	100 (90.0-100%)
LV	80.0 (28.4-99.5%)	100 (89.4-100%)	100 (39.8-100%)	97.1 (84.7-99.9%)	100 (39.8-100%)	97.1 (84.7-99.9%)	80 (28.4-99.5%)	100 (89.4-100%)
RVOT	66.7 (22.3-95.7%)	93.1 (77.2-99.2%)	66.7 (22.3-95.7%)	93.1 (77.2-99.2%)	66.7 (22.3-95.7%)	93.1 (77.2-99.2%)	66.7 (22.3-95.7%)	93.1 (77.2-99.2%)
LVOT	100 (39.8-100%)	92.9 (76.5-99.1%)	66.7 (22.3-95.7%)	100 (86.8-100%)	66.7 (22.3-95.7%)	100 (86.8-100%)	100 (39.8-100%)	92.9 (76.5-99.1%)
PV	66.7 (9.4-99.2%)	94.1 (71.3-99.9%)	6.79 (43.0-99.2%)	94.1 (71.3-99.9%)	66.7 (9.4-99.2%)	94.1 (71.3-99.9%)	66.7 (9.4-99.2%)	94.1 (71.3-99.9%)
MPA	50 (6.8-93.2%)	96 (79.6-99.9%)	66.7 (9.4-99.2%)	92.3 (74.9-99.1%)	66.7 (9.4-99.2%)	92.3 (74.9-99.1%)	50 (6.8-93.2%)	96 (79.6-99.9%)
RPA	50 (1.3-98.7%)	90 (68.3-98.8%)	33.3 (0.8-90.6%)	94.7 (74.0-99.9%)	33.3 (0.8-90.6%)	94.7 (74.0-99.9%)	50 (1.3-98.7%)	90 (68.3-98.8%)
LPA	50 (1.3-98.7%)	89.5 (66.9-98.7%)	33.3 (0.8-90.6%)	94.4 (72.7-99.9%)	33.3 (84.0-90.6%)	94.4 (72.7-99.9%)	50 (1.3-98.7%)	89.5 (66.9-98.7%)
Ao VALVE	33.3 (0.8-90.6%)	100 (83.2-100%)	100 (2.5-100%)	90.9 (70.8-98.9%)	100 (2.5-100%)	90.9 (70.8-98.9%)	33.3 (0.8-90.6%)	83.2 (83.2-100%)
Ao ROOT	50 (11.8-88.2%)	100 (87.7-100%)	100 (29.2-100%)	90.3 (74.2-98%)	100 (29.2-100%)	90.3 (74.2-98.0%)	50 (11.8-88.2%)	100 (87.7-100%)
AV CONCORDANCE	100	NC	NC	NC	NC	NC	NC	NC
VA CONCORDANCE	75 (19.4-99.4%)	96.6 (82.2-99.9%)	75 (19.4-99.4%)	96.6 (82.2-99.9%)	75 (19.4-99.4%)	96.6 (82.2-99.9%)	75 (19.4-99.4%)	96.6 (82.2-99.9%)
Ao ARCH	100 (15.8-100%)	100 (59.0-100%)	100 (15.8-100%)	100 (59.0-100%)	100 (15.8-100%)	100 (59.0-100%)	100 (15.8-100%)	100 (59.0-100%)
DUCTAL ARCH	100	NC	NC	NC	NC	NC	NC	NC
OTHER	100	NC	NC	NC	NC	NC	NC	NC

Table 8: distribution of “non-visible” indices in the general population. At the top of the columns, first letter refers to micro-CT and second letter to autopsy

INDEX	ND/N	ND/AB	N/ND	AB/ND	ND/ND
ABDOMINAL SITUS	0	0	0	0	48
CARDIAC POSITION	0	0	0	0	48
SVR	16	0	14	0	13
PVR	4	0	19	0	24
RA	3	0	3	0	0
LA	3	0	2	0	0
CORONARY SINUS	2	0	8	0	38
ATRIAL SEPTUM	5	0	11	3	4
TV	3	0	3	1	2
MV	4	0	5	1	1
VENTRICULAR SEPTUM	0	0	5	3	4
RV	0	0	10	0	0
LV	0	0	9	1	0
RVOT	0	1	11	1	0
LVOT	0	1	13	2	0
PV	0	1	19	0	7
MPA	0	0	13	2	4
RPA	1	0	17	2	6
LPA	1	0	18	2	6
Ao VALVE	0	0	16	2	7
Ao ROOT	0	0	11	1	3
AV CONCORDANCE	0	0	15	0	2
VA CONCORDANCE	0	0	12	0	2
Ao ARCH	0	1	13	2	23
DUCTAL ARCH	0	0	13	1	32
OTHER	0	1	7	0	40

Table 9: analysis of primary end point in the subgroup of “challenging specimen”

	GOLD STANDARD=AUTOPSY				GOLD STANDARD=MICRO-CT			
	SENSITIVITY (%) (95% CI)	SPECIFICITY (%) (95% CI)	PPV (%) (95% CI)	NPV (%) (95% CI)	SENSITIVITY (%) (95% CI)	SPECIFICITY (%) (95% CI)	PPV (%) (95% CI)	NPV (%) (95% CI)
SVR	33.3 (4.3-77.7%)	55.6 (30.8-78.5%)	20.2 (0.5-55.6%)	71.4 (41.9-91.6%)	20.0 (2.5-55.6%)	71.4 (41.9-91.6%)	33.3 (4.3-77.7%)	55.6 (30.8-78.5%)
PVR	50.1 (0.3-98.7%)	59 (36.4-79.3%)	10 (0.3-44.5%)	92.9 (66.1-99.8%)	10.0 (0.3-44.5%)	92.9 (66.1-99.8%)	50.0 (1.3-98.7%)	59.1 (36.4-79.3%)
RA	90.5 (69.6-98.8%)	0 (0-70.8%)	86.4 (65.1-97.1%)	0 (0-84.2%)	86.4 (65.1-97.1%)	0 (0-84.2%)	90.5 (69.6-98.8%)	0 (0-70.8%)
LA	90.9 (70.8-98.9%)	0 (0-84.2%)	90.9 (70.8-98.9%)	0 (0-84.2%)	90.9 (70.8-98.9%)	0 (0-84.2%)	90.9 (70.8-98.9%)	0 (0-84.2%)
CORONARY SINUS	NC	NC	NC	NC	NC	NC	NC	NC
ATRIAL SEPTUM	84.6 (54.6-98.1%)	27.3 (6.0-61%)	57.9 (33.5-79.7%)	60.0 (14.7-94.7%)	57.9 (33.5-79.7%)	60.0 (14.7-94.7%)	84.6 (54.6-98.1%)	27.3 (6.0-61%)
TV	88.9 (65.3-98.6%)	33.3 (4.33-77.7%)	80.0 (56.3-94.3%)	50.0 (6.8-93.2%)	80.0 (56.3-94.3%)	50.0 (6.8-93.2%)	88.9 (65.3-98.6%)	33.3 (4.3-77.7%)
MV	82.4 (56.6-96.2%)	14.3 (0.36-57.9%)	70.0 (45.7-88.1%)	25.0 (0.6-80.6%)	70.0 (45.7-88.1%)	25.0 (0.6-80.6%)	82.4 (56.6-96.2%)	14.3 (0.4-57.9%)
VENTRICULAR SEPTUM	100 (79.4-100%)	12.5 (0.31-52.7%)	69.6 (47.1-86.8%)	100 (2.5-100%)	69.6 (47.1-86.8%)	100 (2.5-100%)	100 (79.4-100%)	12.5 (0.3-52.7%)
RV	100	NC	58.3	NC	58.3	NC	100	NC
LV	100	NC	41.7	NC	58.3	NC	100	NC
RVOT	100	NC	54.2	NC	54.1	NC	100	NC
LVOT	100	NC	41.7	NC	58.3	NC	100	NC
PV	100 (66.4-100%)	33.3 (11.8-61.6%)	47.4 (24.4-71.1%)	100 (47.8-100%)	47.4 (24.4-71.1%)	100 (47.8-100%)	100 (66.4-100%)	33.3 (11.8-61.6%)
MPA	100 (69.2-100%)	21.4 (4.7-50.8%)	47.6 (25.7-70.2%)	100 (29.2-100%)	47.6 (25.7-70.2%)	100 (29.2-100%)	100 (69.2%-100%)	21.4 (4.7-50.8%)
RPA	100 (59.0-100%)	29.4 (10.3-56.0%)	36.8 (16.0-61.6%)	100 (47.8-100%)	36.8 (16.3-61.6%)	100 (47.8-100%)	100 (59.0-100%)	29.4 (10.3-56%)
LPA	100 (59.0-100%)	29.4 (10.3-56.0%)	36.8 (16.3-61.6%)	100 (47.8-100%)	36.8 (16.3-61.6%)	100 (47.8-100%)	100 (59.0-100%)	29.4 (10.3-56%)
Ao VALVE	100 (71.5-100%)	38.5 (13.9-68.4%)	57.9 (33.5-79.7%)	100 (47.8-100%)	57.9 (33.5-79.7%)	100 (47.8-100%)	100 (71.5-100%)	38.5 (13.9-68.4%)
Ao ROOT	100 (75.3-100%)	27.3 (6.0-61.0%)	61.9 (38.4-81.9%)	100 (29.2-100%)	61.9 (38.4-81.9%)	100 (29.2-100%)	100 (75.3-100%)	27.3 (6.0-61%)
AV CONCORDANCE	100 (66.4-100%)	13.3 (1.7-40.5%)	40.9 (20.7-63.6%)	100 (15.8-100%)	40.9 (20.7-63.6%)	100 (15.8-100%)	100 (66.4-100%)	13.3 (1.7-40.5%)
VA CONCORDANCE	100 (75.3-100%)	18.2 (2.3-51.8%)	59.1 (36.4-79.3%)	100 (15.8-100%)	59.9 (36.4-79.3%)	100 (15.8-100%)	100 (75.3-100%)	18.2 (2.3-51.8%)
Ao ARCH	75.0 (19.4-99.4%)	65.0 (40.8-84.6%)	30.0 (6.7-65.2%)	92.9 (66.1-99.8%)	30.0 (6.7-65.2%)	92.9 (66.1-99.8%)	75 (19.4-99.4%)	65 (40.8-84.6%)
DUCTAL ARCH	NC	NC	NC	NC	NC	NC	NC	NC
OTHER	100 (2.5-100%)	91.3 (72.0-98.9%)	33.3 (0.8-90.6%)	100 (83.9-100%)	33.3 (0.8-90.6%)	100 (83.9-100%)	100 (2.5-100%)	91.3 (72.0-98.9%)

Table 10: analysis of secondary end point in the subgroup of “challenging specimens”

	GOLD STANDARD=AUTOPSY				GOLD STANDARD=MICRO-CT			
	SENSITIVITY (%) (95% CI)	SPECIFICITY (%) (95% CI)	PPV (%) (95% CI)	NPV (%) (95% CI)	SENSITIVITY (%) (95% CI)	SPECIFICITY (%) (95% CI)	PPV (%) (95% CI)	NPV (%) (95% CI)
SVR	NC	NC	NC	NC	NC	20	NC	NC
PVR	NC	NC	NC	10	NC	10	NC	NC
RA	NC	89.5	NC	89.5	NC	89.5	NC	NC
LA	NC	90.4	NC	95	NC	95	NC	NC
CORONARY SINUS	NC	NC	NC	NC	NC	NC	NC	NC
ATRIAL SEPTUM	100 (29.2-100%)	100 (63.1-100%)	100 (29.2-100%)	100 (63.1-100%)	100 (29.2-100%)	100 (63.1-100%)	100 (29.2-100%)	100 (63.1-100%)
TV	80.0 (28.4-99.5%)	100 (71.5-100%)	100 (39.8-100%)	91.7 (61.5-99.8%)	100 (39.8-100%)	91.7 (61.5-99.8%)	80.0 (28.4-99.5%)	100 (71.5-100%)
MV	100 (39.8-100%)	100 (69.2-100%)	100 (39.8-100%)	100 (69.2-100%)	100 (39.8-100%)	100 (69.2-100%)	100 (39.8-100%)	100 (69.2-100%)
VENTRICULAR SEPTUM	87.5 (47.3-99.7%)	62.5 (24.5-91.5%)	70.0 (34.8-93.3%)	83.3 (35.9-99.6%)	70.0 (34.8-93.3%)	83.3 (35.9-99.6%)	87.5 (47.3-99.7%)	62.5 (24.5-91.5%)
RV	100 (2.5-100%)	100 (75.3-100%)	100 (2.5-100%)	100 (75.3-100%)	100 (2.5-100%)	100 (75.3-100%)	100 (2.5-100%)	100 (75.3-100%)
LV	100 (15.8-100%)	100 (73.5-100%)	100 (15.8-100%)	100 (73.5-100%)	100 (15.8-100%)	100 (73.5-100%)	100 (15.8-100%)	100 (73.5-100%)
RVOT	75.0 (19.4-99.4%)	88.9 (51.8-99.7%)	75.0 (19.4-99.4%)	88.9 (51.8-99.7%)	75.0 (19.4-99.4%)	88.9 (51.8-99.7%)	75.0 (19.4-99.4%)	88.9 (51.8-99.7%)
LVOT	100 (15.8-100%)	87.5 (47.3-99.7%)	66.7 (9.4-99.2%)	100 (59.0-100%)	66.7 (9.4-99.2%)	100 (59.0-100%)	100 (15.8-100%)	87.5 (47.3-99.7%)
PV	100 (15.8-100%)	100 (59.0-100%)	100 (15.8-100%)	100 (59.0-100%)	100 (15.8-100%)	100 (59.0-100%)	100 (15.8-100%)	100 (59.0-100%)
MPA	100 (15.8-100%)	100 (63.1-100%)	100 (15.8-100%)	100 (63.1-100%)	100 (15.8-100%)	100 (63.1-100%)	100 (15.8-100%)	100 (63.1-100%)
RPA	100 (2.5%-100%)	83.3 (35.9-99.6%)	50.0 (1.3-98.7%)	100 (47.8-100%)	50.0 (1.3-98.7%)	100 (47.8-100%)	100 (2.5-100%)	83.3 (35.9-99.6%)
LPA	100 (2.5%-100%)	83.3 (35.9-99.6%)	50.0 (1.3-98.7%)	100 (47.8-100%)	50.0 (1.3-98.7%)	100 (47.8-100%)	100 (2.5-100%)	83.3 (35.9-99.6%)
Ao VALVE	NC	100	NC	81.8	NC	81.8	NC	NC
Ao ROOT	NC	100	NC	84.6	NC	84.6	NC	NC
AV CONCORDANCE	NC	100	NC	NC	NC	100	NC	NC
VA CONCORDANCE	50.0 (1.3-98.7%)	90.9 (58.7-99.8%)	50 (1.3-98.7%)	90.9 (58.7-99.8%)	50.0 (1.3-98.7%)	90.9 (58.7-99.8%)	50.0 (1.3-98.7%)	90.9 (58.7-99.8%)
Ao ARCH	100 (2.5-100%)	100 (15.8-100%)	100 (2.5-100%)	100 (15.8-100%)	100 (2.5-100%)	100 (15.8-100%)	100 (2.5-100%)	100 (15.8-100%)
DUCTAL ARCH	NC	NC	NC	NC	NC	NC	NC	NC
OTHER	NC	NC	NC	NC	NC	NC	NC	NC

Table 11: distribution of “non-visible” indices in the subgroup of “challenging specimens”. At the top of the columns, first letter refers to CT and second letter to autopsy

INDEX	ND/N	ND/AB	N/ND	AB/ND	ND/ND
1 ABDOMINAL SITUS	0	0	0	0	24
2 CARDIAC POSITION	0	0	0	0	24
3 SVR	4	0	8	0	10
4 PVR	1	0	9	0	13
5 RA	2	0	3	0	0
6 LA	2	0	2	0	0
7 CORONARY SINUS	0	0	4	0	20
8 ATRIAL SEPTUM	2	0	6	2	3
9 TV	2	0	3	1	2
10 MV	3	0	5	1	1
11 VENTRICULAR SEPTUM	0	0	5	2	1
12 RV	0	0	10	0	0
13 LV	0	0	9	1	0
14 RVOT	0	0	10	1	0
15 LVOT	0	0	13	1	0
16 PV	0	0	10	0	5
17 MPA	0	0	9	2	3
18 RPA	0	0	10	2	5
19 LPA	0	0	10	2	5
20 AoV	0	0	8	0	5
21 Ao ROOT	0	0	8	0	3
22 AV CONCORDANCE	0	0	13	0	2
23 VA CONCORDANCE	0	0	9	0	2
24 Ao ARCH	0	1	6	1	13
25 DUCTAL ARCH	0	0	7	1	16
26 OTHER	0	1	1	0	22

Table 12: “non-diagnostic” indices

CASE	INDICES “NON-VISIBLE” IN CT BUT VISIBLE IN AUTOPSY	INDICES “NON-VISIBLE” IN AUTOPSY BUT VISIBLE IN CT	INDICES “NON-VISIBLE” IN BOTH CT AND AUTOPSY
C1	/	SVR, PVR	CS, ventricular septum, ductal arch, other
C2	/	SVR, PVR, CS, atrial septum	ductal arch, other
C3	RVOT, LVOT, PV	SVR, atrial septum, aortic arch	PVR, CS, MPA, RPA, LPA, ductal arch, other
C4	/	SVR, PVR, atrial septum, aortic arch	CS, ventricular septum, ductal arch, other
C5	/	SVR, PVR, atrial septum, aortic valve	CS, ventricular septum, ductal arch, other
C6 *	/	SVR, PVR, atrial septum	CS, ductal arch, other
C7*	/	SVR, PVR, atrial septum, RV, LV, RVOT, LVOT, PV, MPA, RPA, LPA, AoV, Ao root, AV and VA concordance, Ao arch	CS, ductal arch, other
C8*	/	SVR, PVR, atrial septum, PV	CS, ventricular septum, ductal arch, other
C9	/	SVR, PVR, atrial septum, ductal arch	CS, ventricular septum, other
C10*	/	SVR, PVR, RV, LV, RVOT, LVOT, PV, MPA, RPA, LPA, AoV, Ao root, AV and VA concordance, Ao arch	CS, ductal arch, other
C11*	Other (small MAPCAs from MPA)	SVR, PVR, CS, LVOT, MPA, RPA, LPA, AV concordance, ductal arch	Ao arch
C12*	SVR	LVOT, MPA, RPA, LPA, AV concordance	PVR, CS, Ao arch, ductal arch, other
C13*	/	PVR, CS, LVOT, AV concordance, ductal arch, other (coronary arteries)	Ao arch
C15*	/	Ventricular septum, RV, LV, RVOT, LVOT	SVR, PVR, CS, atrial septum, TV, MV, , PV, MPA, RPA, LPA, AoV, Ao root, VA concordance, Ao arch, ductal arch, other
C16*	SVR		PVR, CS, Ao arch, ductal arch, other
C17*	/	RA, LA, RPA, LPA, ductal arch	CS
C19*	/	SVR, PVR, PV, MPA, RPA, LPA, Ao valve, Ao arch, ductal arch	CS, other
C20*	SVR, atrial septum, MV, TV, Ao arch		PVR, CS, ductal arch, other
C21*	/	RA, atrial septum, MV, TV, ventricular septum, RV, LV, RVOT, LVOT, AV and VA concordance	SVR, PVR, CS, PV, MPA, RPA, LPA, AoV, Ao root, Ao arch, ductal arch, other
C22*	/	MPA, RPA, LPA	SVR, PVR, CS, Ao arch, ductal arch, other
C23	/	PVR, LPA	CS, Ao arch, ductal arch, other
C25	SVR	RPA, LPA	PVR, CS, PV, aortic valve, Ao arch, ductal arch, other
C27*	/	Ao valve	SVR, PVR, CS, RPA, LPA, Ao arch, ductal arch, other
C28*	SVR, PVR, RA, LA, atrial septum, MV, TV,	PV, Ao valve, Ao arch, ductal arch	CS, AV concordance, other
C29	SVR, PVR	Ao arch, ductal arch, other	CS
C30	SVR, atrial septum	ductal arch	PVR, CS, other
C31	SVR	Ao arch	PVR, CS, ductal arch, other
C32*	/	RA, LA, AV concordance	SVR, PVR, CS, Ao arch, ductal arch, other
C33*	RA, LA,	MV, ventricular septum, RV, LV, RVOT, LVOT, AV and VA concordance	SVR, PVR, CS, atrial septum, PV, RPA, LPA, Ao valve, Ao arch, ductal arch, other
C34	PVR, CS, atrial septum, TV, MV	/	other
C35*	MV	RV, LV, RVOT, LVOT	SVR, PVR, CS, atrial septum, TV, PV, MPA, RPA, LPA, Ao valve, Ao root, AV and VA concordance, , Ao arch, ductal arch, other
C36	SVR, PVR	other	CS, PV, aortic valve, Ao arch, ductal arch
C37	CS	Ventricular septum, LVOT, PV, MPA, RPA, LPA, aortic valve, aortic root, av and va concordance, aortic arch, ductal arch	SVR, PVR, other
C38*	/	atrial septum, MV, TV, ventricular septum, RV, LV, RVOT, LVOT, PV, MPA, RPA, LPA, Ao valve, Ao root, AV and VA concordance, Ao arch	SVR, PVR, CS, ductal arch, other
C40	SVR, atrial septum	CS, PV, RPA, LPA, Ao valve	PVR, Ao arch, ductal arch, other
C41	SVR	CS, PV, MPA, RPA, LPA, Ao valve, ao root, av and va concordance	PVR, Ao arch, ductal arch, other
C42	/	PVR	SVR, CS, other
C43	SVR	PVR, MPA, RPA, LPA, Ao valve, ao root, other	CS, Ao arch, ductal arch
C44	SVR	PVR, PV, RPA, LPA, Ao valve, ductal arch, other	CS, aortic arch
C45*	/	SVR, PVR, CS, atrial septum, MV, ventricular septum, RV, LV, RVOT, LVOT, PV, MPA, RPA, LPA, Ao valve, Ao root, AV and VA concordance, Ao arch, ductal arch	other
C46	SVR	PV, MPA, RPA, LPA, Ao valve, ao root, va concordance	PVR, CS, Ao arch, ductal arch, other
C47*	/	RVOT, LVOT, MPA, RPA, LPA, Ao root, VA concordance, ductal arch	SVR, PVR, CS, PV, Ao valve, Ao arch, other
C48*	/	CS, atrial septum, TV, MV, ventricular septum, RV,	SVR, PVR, Ao arch, ductal arch, other

		LV, RVOT, LVOT, PV, MPA, RPA, LPA, Ao valve, Ao root, AV and VA concordance	
C51	/	PV, Ao valve	SVR, PVR, CS, Ao arch, ductal arch, other
C52*	/	SVR, PVR, atrial septum, TV, MV, ventricular septum, RV, LV, RVOT, LVOT, PV, MPA, RPA, LPA, Ao valve, Ao root, AV and VA concordance, Ao arch, ductal arch	CS, other
C53	/	PVR, CS, PV, Ao valve, Ao arch, ductal arch, other	/
C54	SVR	PV, Ao valve, other	PVR, CS, Ao arch, ductal arch
C55	SVR, RA, LA	Aortic arch	PVR, CS, atrial septum, ductal arch, other

“*” refers to challenging specimens . CS: coronary sinus

Table 13: critical data of the project

EPIDEMIOLOGICAL INFORMATION	
N.	55
Available for comparison	48/55 (87.3%)
Heart	31/48 (64.6%)
Heart and lungs	17/48 (35.4%)
GA at prenatal diagnosis	16.3±2.8 w (12 ⁺⁴ -21 ⁺⁴ w)
GA at TOP	17.0±2.9 w (12 ⁺⁵ -21 ⁺⁶ w)
Dimension	
Longitudinal diameter	1.38±0.58 cm (0.40-3.00 cm)
Transverse diameter	1.12±0.45 cm (0.40-2.10 cm)
Weight	2.66±2.92 g (0.13-13.90 g)
CHD	29/48 (60.4 %)
Simple	7/29 (24.1%)
Complex	22/29 (75.9%)
Associated to chromosomal or extra-cardiac anomalies	27/29 (93.1%)
Normal heart	19/48 (39.6%)
Associated to chromosomal or extra-cardiac anomalies	18/19 (94.7%)
CHALLENGING SPECIMENS	
	24/48 (50.0%)
CHD	15/24 (62.5 %)
Simple CHD	2/15 (13.3%)
Complex CHD	13/15 (86.7%)
Associated to chromosomal or extra-cardiac anomalies	14/15 (93.3%)
Normal heart	9/24 (37.5%)
Associated to chromosomal or extra-cardiac anomalies	8/9 (88.9%)
STATISTICAL DATA	
GENERAL DIAGNOSIS	
Feasibility of autopsy	37/48 (77.1%)
Feasibility of micro-CT	48/48 (100%)
Agreement in diagnoses	28/37 (75.6%)
GOLD STANDARD: AUTOPSY	
PRIMARY END POINT	
Agreement	73.4% (95% CI, 71.0-75.8%)
Sensitivity	92.8% (95%CI, 90.9-94.8%)
Specificity	51.8% (95% CI, 48.1-55.5%)
PPV	67.1% (95% CI, 37.6-96.4%)
NPV	87.2% (95% CI, 83.8-90.6%)
SECONDARY END POINT	
Agreement	93.3% (95% CI, 91.3-95.3%)
Sensitivity	97.3% (95% CI, 95.9-98.7%)
Specificity	68.3% (95% CI, 58.5-78.1%)
PPV	95.1% (95% CI, 93.3-96.9%)
NPV	80.0% (95% CI, 71.0-89.0%)
Apparent advantage of micro-CT	86.1%
GOLD STANDARD: AUTOPSY; SUBGROUP OF CHALLENGING SPECIMENS	
PRIMARY END POINT	
Agreement	65.9% (95% CI, 62.2-69.6%)
Sensitivity	92.8% (95% CI, 89.7-95.9%)
Specificity	47.8% (95% CI, 43.1-52.5%)
PPV	54.3% (95% CI, 49.6-59.0%)
NPV	90.9% (95% CI, 87.0-94.8%)
SECONDARY END POINT	
Agreement	91.8% (95% CI 88.4-95.2%)
Sensitivity	95.7% (95% CI 92.8-98.6%)
Specificity	75.6% (95% CI 63.6-87.9%)
PPV	94.2% (95% CI 90.7-97.3%)
NPV	81.0% (95% CI 69.2-92.8%)
Apparent advantage of micro-CT	91.5%
GOLD STANDARD MICRO-CT	
PRIMARY END POINT	
Agreement	73.4% (95% CI, 71.0-75.8%)
Sensitivity	67.1% (95% CI, 37.6-96.4%)
Specificity	87.2% (95% CI, 83.8-90.6%)
PPV	92.8% (95% CI, 90.9-94.8%)
NPV	51.8% (95% CI, 48.1-55.1%)
SECONDARY END POINT	
Agreement	93.3% (95% CI, 91.3-95.3%)
Sensitivity	95.1% (95% CI, 93.3-96.9%)
Specificity	80.0% (95% CI, 71.0-89.0%)
PPV	68.3% (95% CI, 58.5-78.1%)
NPV	97.2% (95% CI, 95.9-98.7%)
Apparent advantage of autopsy	13.9%
GOLD STANDARD MICRO-CT; SUBGROUP OF CHALLENGING SPECIMENS	
PRIMARY END POINT	
Agreement	65.9% (95% CI, 62.2-69.6%)

Sensitivity	54.3% (95% CI, 49.6-59.0%)
Specificity	90.9% (95% CI, 87.0-94.8%)
PPV	92.8% (95% CI, 89.7-95.9%)
NPV	47.8% (95% CI, 43.1-52.5%)
SECONDARY END POINT	
Agreement	91.8% (95% CI, 88.4-95.2%)
Sensitivity	94.2% (95% CI, 90.7-97.3%)
Specificity	81.0% (95% CI, 69.2-92.8%)
PPV	95.7% (95% CI, 92.8-98.6%)
NPV	75.6% (95% CI, 63.6-87.9%)
Apparent advantage of autopsy	8.5%

FIGURE LEGEND

Figure 1: case 19, normal heart

Figure 2: case 10, atrioventricular septal defect

Figure 3: case 5, hypoplastic left heart syndrome

Figure 4: case 40, tricuspid atresia (associated to ventricular septal defect and transposed great arteries)

Figure 5: case 6, pulmonary atresia/ventricular septal defect

Figure 1

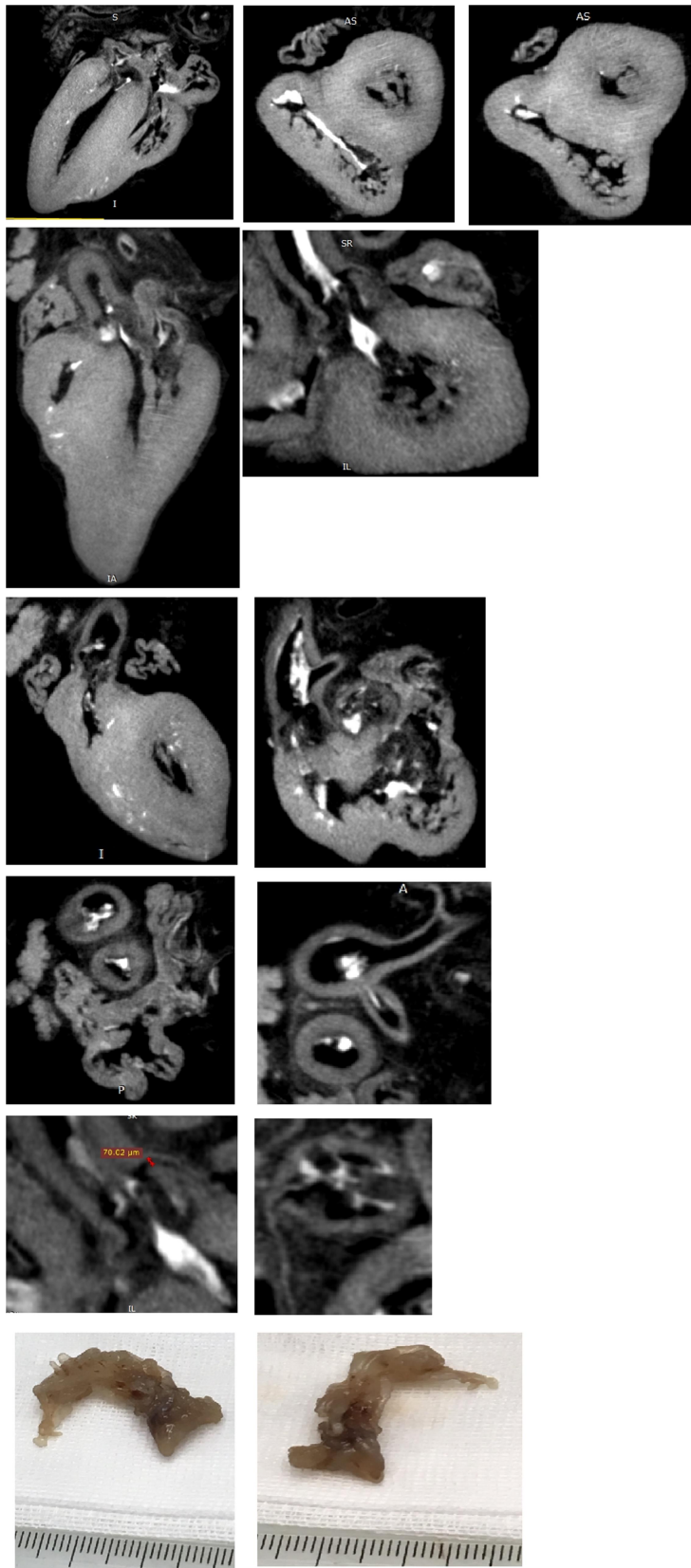


Figure 2

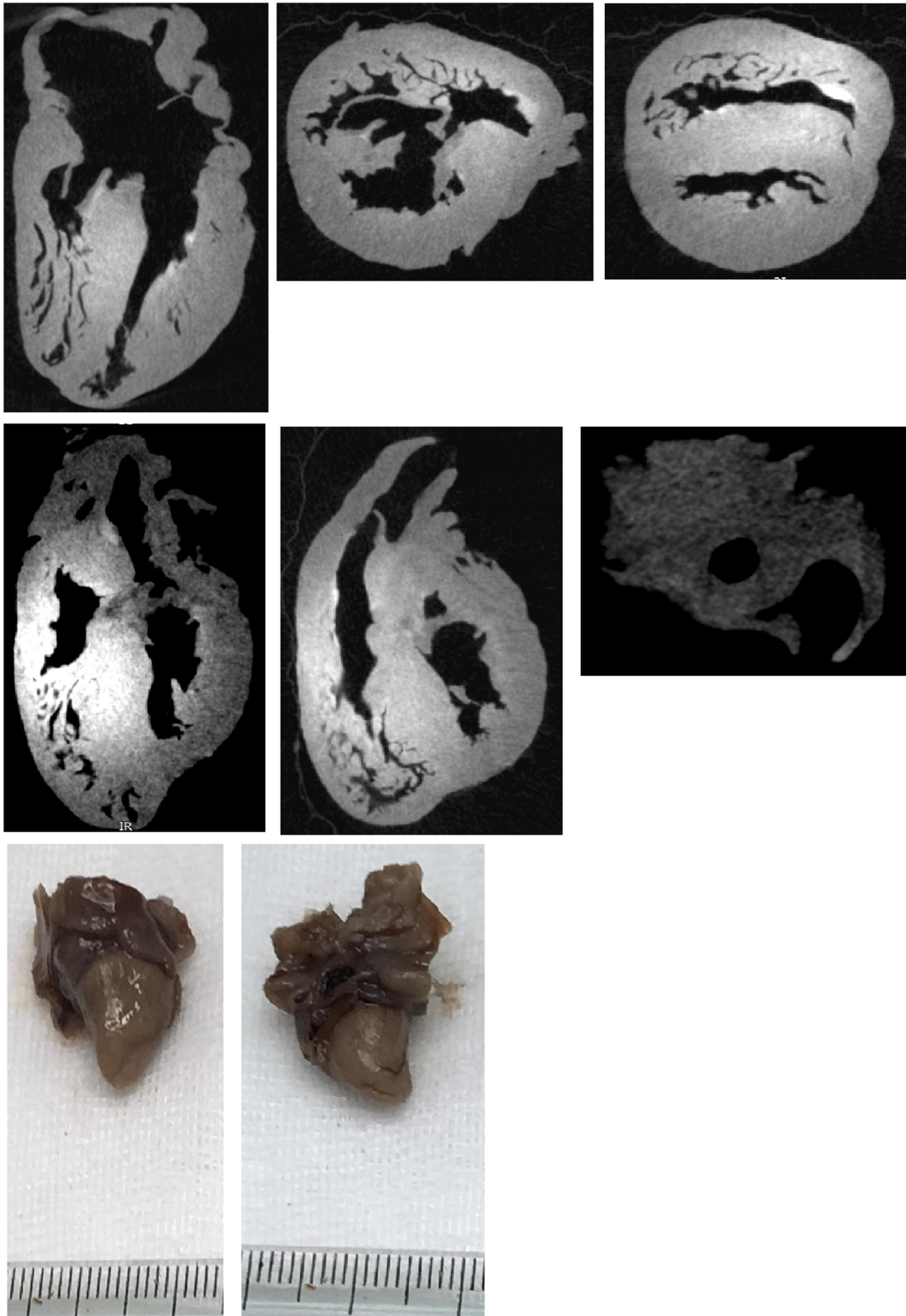


Figure 3

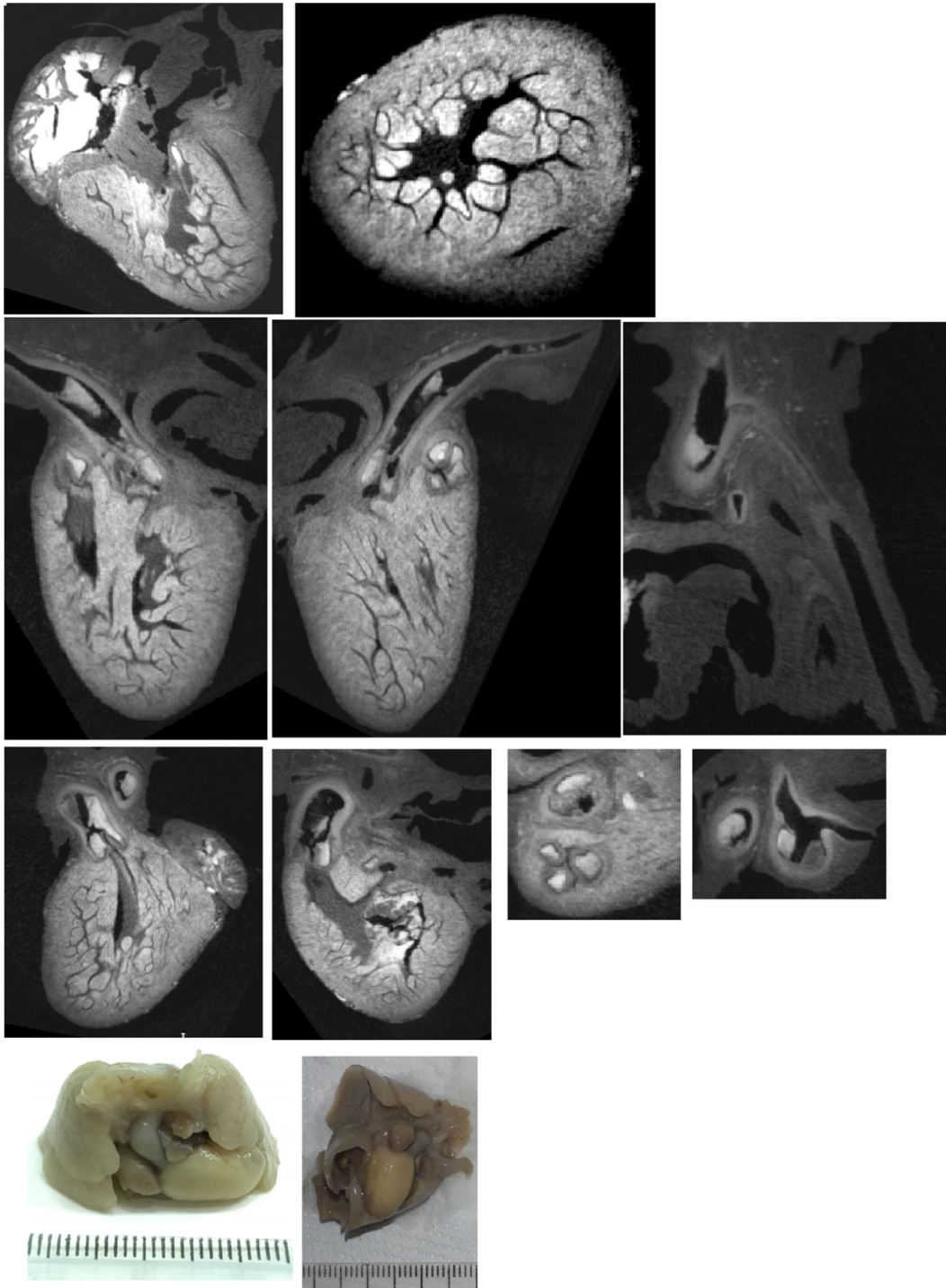


Figure 4



Figure 5

